Available online at www.sciencedirect.com
ScienceDirect
Sedimentary Geology 199 (2007) 65–89
Sedimentary Geology
www.elsevier.com/locate/sedgeo

Late Quaternary co-seismic sedimentation in the Sea of Marmara's deep basins

Christian Beck [a,*], Bernard Mercier de Lépinay [b], Jean-Luc Schneider [c], Michel Cremer [c], Namik Çağatay [d], Evrard Wendenbaum [a,b], Sébastien Boutareaud [a,c], Guillemette Ménot [e], Sabine Schmidt [c], Olivier Weber [c], Kadir Eris [d], Rolando Armijo [f], Bertrand Meyer [f], Nicolas Pondard [f], Marc-André Gutscher [g], and the MARMACORE Cruise Party, J.-L. Turon [c], L. Labeyrie [h], E. Cortijo [h], Y. Gallet [f], Hélène Bouquerel [f], N. Gorur [i], A. Gervais [c], M.-H. Castera [c], L. Londeix [c], A. de Rességuier [c], A. Jaouen [j]

[a] *Laboratoire de Géodynamique des Chaînes Alpines, U.M.R. C.N.R.S. 5025, U.F.R. C.I.S.M. Université de Savoie, 73 376 Le Bourget du Lac, France*
[b] *Géosciences Azur, U.M.R. C.N.R.S. 6526, Université de Nice-Sophia-Antipolis, 06 560 Valbonne, France*
[c] *Département de Géologie et Océanographie, U.M.R. C.N.R.S. 5805, Université de Bordeaux I, 33 405 Talence Cedex, France*
[d] *Geology and Mining Faculty, Istanbul Technical University, (ITU), Maslak Istanbul, Turkey*
[e] *Lamont-Doherty Earth Observatory, Colombia University, Woods Hole, Massachusetts. presently at CEREGE, UMR-6635, Europole de l'Arbois, BP80, 13545 Aix-en-Provence cedex 4, France*
[f] *Institut de Physique du Globe de Paris, CNRS UMR 7578, Université Pierre et Marie Curie, 75 252 Paris, France*
[g] *I.U.E.M., Domaines Océaniques, U.M.R. C.N.R.S. 6538, Université de Bretagne Occidentale, 29 280 Plouzané, France*
[h] *Laboratoire des Sciences du Climat et de l'Environnement, U.M.R. C.N.R.S.-C.E.A. 1572, 91 198 Gif-sur-Yvette, France*
[i] *Scientific and Technical Research Council of Turkey (TUBITAK), Marmara Research Center (MAM), Earth and Marine Research Institute, Kocaeli, Turkey*
[j] *Institut Paul-Emile Victor, Technopole Brest-Iroise, BP 75, 29 280 Plouzané, France*

Abstract

The deep, northern, part of the Sea of Marmara (northwestern Turkey) is composed of several aligned, actively subsiding, basins, which are the direct structural and morphological expression of the North-Anatolian Fault's northern branch. The last 20 kyr of their sedimentary fill (non-marine before 12 kyr BP) have been investigated through giant piston coring onboard R/V MARION-DUFRESNE (MARMACORE Cruise, 2001) and by chirp sub-bottom profiler onboard R/V ATALANTE during MARMARASCARPS Cruise (2002). Especially during the lacustrine stage, the infilling of the deep basins (Tekirdağ, Central, Kumburgaz, and Çinarcic Basins; up to 1250-m depth) was dominated by turbidites (with coarse mixed siliciclastic and bioclastic basal parts), intercalated in "hemipelagic-type" fine-grained calcareous and slightly siliceous clays. Often the turbidites show strong segregation and a sharp boundary between a coarse lower part and a suspended-load upper part. In the Central Basin, 8 m of a unique sedimentary event include a 5 to 8-m thick "homogenite" well imaged on seismic profiles. The latter is interpreted as related to a major – possibly earthquake-triggered – tsunami effect, as described in the Eastern Mediterranean by Kastens and Cita [Kastens K. and Cita M.B., 1981. Tsunami-induced sediment transport in the abyssal Mediterranean Sea. Geological Society of

* Corresponding author. Tel.: +33 4 79 75 87 05; fax: +33 4 79 75 87 77.
E-mail address: beck@univ-savoie.fr (C. Beck).

0037-0738/$ - see front matter
doi:10.1016/j.sedgeo.2005.12.031

America Bulletin, 92:845–857]. In the marine (Holocene) upper part of the sedimentary fill, repeated to-and-from structures, affecting silt or fine sand, are evidencing seiche-like effects and, thus, earthquake triggering. Detailed correlations between two deep coring sites (at 1250 m and 1200 m) indicate more than 100% over-thickening in the deepest one; this implies specific processes of distribution of terrigenous input by dense currents (high kinetic energy, seiche effects, complex reflections on steep slopes). The peculiar sedimentary fill of the Sea of Marmara's Central Basin is interpreted as a direct consequence of the strong seismic activity, (and, by extrapolation, to the whole set of deep basins). This imprint is more significant below the base of the Holocene, as environmental conditions favoured marginal accumulation (especially on the southern shelf) of large amounts of erosion products available for mass wasting.

Keywords: Sea of Marmara; Late Quaternary; Cores; High resolution seismic; Earthquakes; Turbidites; Homogenites

1. Introduction

Since the results of diverse investigations conducted on both marine and lacustrine fills, possible sedimentary effects of strong earthquakes have been described and progressively taken into account as paleoseismic indicators (Kuenen, 1958; Sims, 1973, 1975; Ben-Menahem, 1976; Field et al., 1982; Séguret et al., 1984; Seilacher, 1984; Doig, 1985; El-Isa and Mustafa, 1986; Anand and Jain, 1987; Plaziat et al., 1988; Adams, 1990; Doig, 1991; Tuttle and Seeber, 1991; Piper et al., 1992; Roep and Everts, 1992; Guiraud and Plaziat 1993; Marco and Agnon, 1995; Chapron et al., 1996; Moretti and Tropeano, 1996; Beck et al., 1996; Alfaro et al., 1997; Pratt, 1998; Calvo et al., 1998; Lignier et al., 1998; Chapron, 1999; Chapron et al., 1999). These effects and their sedimentary records appear robust in isolated marine basins and large lakes, submitted to significant seismo-tectonic activity (Hempton and Dewey, 1983; Siegenthaler et al., 1987; Ringrose, 1989; Van Loon et al., 1995; Syvitski and Schafer, 1996; Mörner, 1996; Chapron et al., 1999; Shiki et al., 2000; Gorsline et al., 2000; De Batist et al., 2002; Arnaud et al., 2002; Beck, in press). During the last decade, investigations made attempts to constrain paleoseismological parameters through: 1) analog modelling (Caselles et al., 1997; Moretti et al., 1999); 2) calibration of geotechnical characteristics with seismological parameters (Obermeier, 1989; Obermeier et al., 1991; Audemard and De Santis, 1991; Vittori et al., 1991; Rodriguez-Pascua et al., 2002); 3) delimitation of "paleo-epicentral" area based on sets of synchronous lacustrine records, and use of various correlative indirect evidences (Allen, 1986; Lignier, 2001; Becker et al., 2002, 2005; Carrillo et al., 2006).

In the Mediterranean realm, a major volcanic and seismic event and its consequences (tsunami) have been considered as generating huge sedimentary reworking (Kastens and Cita, 1981; Cita et al., 1996; Cita and Rimoldi, 1997). The resulting deposit appears to specifically fill the deepest parts and to smooth previous relief in deep central-eastern Mediterranean basins. On high resolution seismic reflection profiles, it corresponds to a particular transparent layer called "homogenite" (Kastens and Cita, 1981) or "unifite" (Stanley, 1981). Based on these previous concepts and other investigation results on large intra-mountainous lakes, the deepest part of the Sea of Marmara – which underwent a non-marine episode prior to the last eustatic rise – was investigated as a possible recorder of the frequent strong earthquakes occurring along the North-Anatolian Fault (Mercier de Lépinay et al., 2003; Beck et al., 2003).

2. Geodynamic and paleoenvironmental settings

As evidenced by seismo-tectonic surface studies, seismological investigations, and GPS data, the North-Anatolian Fault is considered as a major active boundary between the Anatolia and Eurasia plates (Armijo et al., 1999; McClusky et al., 2000; Armijo et al., 2002; Flerit et al., 2003) (Fig. 1). In northwestern Turkey, the northern branch of this right-lateral strike-slip fault system is characterised by a set of recent high magnitude earthquakes (Barka and Kadinsky-Cade, 1988; Stein et al., 1997; Barka et al., 2002). A direct consequence of this active structure is the deep northern part of the Sea of Marmara, an East–West trending, 200 km long pull-apart basin, composed of several aligned sub-basins (Figs. 2 and 3). Considered as Pliocene-Quaternary (Wong et al., 1995), the Sea of Marmara syn-tectonic sedimentary fill and its deep substratum have been imaged by seismic reflection surveys (Okay et al., 2000; Carton, 2003; Hirn et al., 2003). The pre-Pliocene substratum involves ophiolitic assemblages, metamorphic and igneous rocks (intrusions and subaerial volcanics), from Paleozoic to Miocene. They represent part of the Pontides (North) and the Taurides (South) peri-Mediterranean belts. Potential terrigenous sources (highest relief) are located on the southern side of the Sea of Marmara and consist

of metamorphic and igneous rocks. The northern border has a lower relief, comprising Tertiary sediments and volcanics. This situation is responsible for higher terrigenous input on the southern shelf (Ergin et al., 1991, 1999). The drainage pattern issued from the southern uplands converges towards tributaries of the Sea of Marmara, while, on the north side, the main hydrologic system flows westwards (Fig. 1), avoiding significant input to the northern shelf.

As the connection between the eastern Mediterranean (Aegean Sea) and the Black Sea through two shallow sills (Dardanelles and Bosphorus), the Sea of Marmara experienced the consequences of the last glacio-eustatic cycle (Ryan et al., 1997; Aksu et al., 1999; Çağatay et al., 2000; Major et al., 2002; Çağatay et al., 2003) and particularly the associated 120-m sea-level rise. Recent paleoenvironmental studies through coring and seismic imagery have been dedicated, by different teams, to the analysis of the Black Sea/Sea of Marmara connection (Ryan et al., 1997). Recent modifications have been investigated through short gravity cores, either in deep basins or in shallow shelf positions (Çağatay et al., 2000, 2003). The lacustrine-to-marine change is considered to have occurred around 12 cal. kyr BP, and is represented either by a sharp boundary in shallow marginal sites, and by a more gradual change in deep-water sites.

Although also concerned with paleoenvironmental aspects, the MARMACORE Cruise's results presented here mainly focus on the search for impacts of seismic activity on recent sedimentary processes.

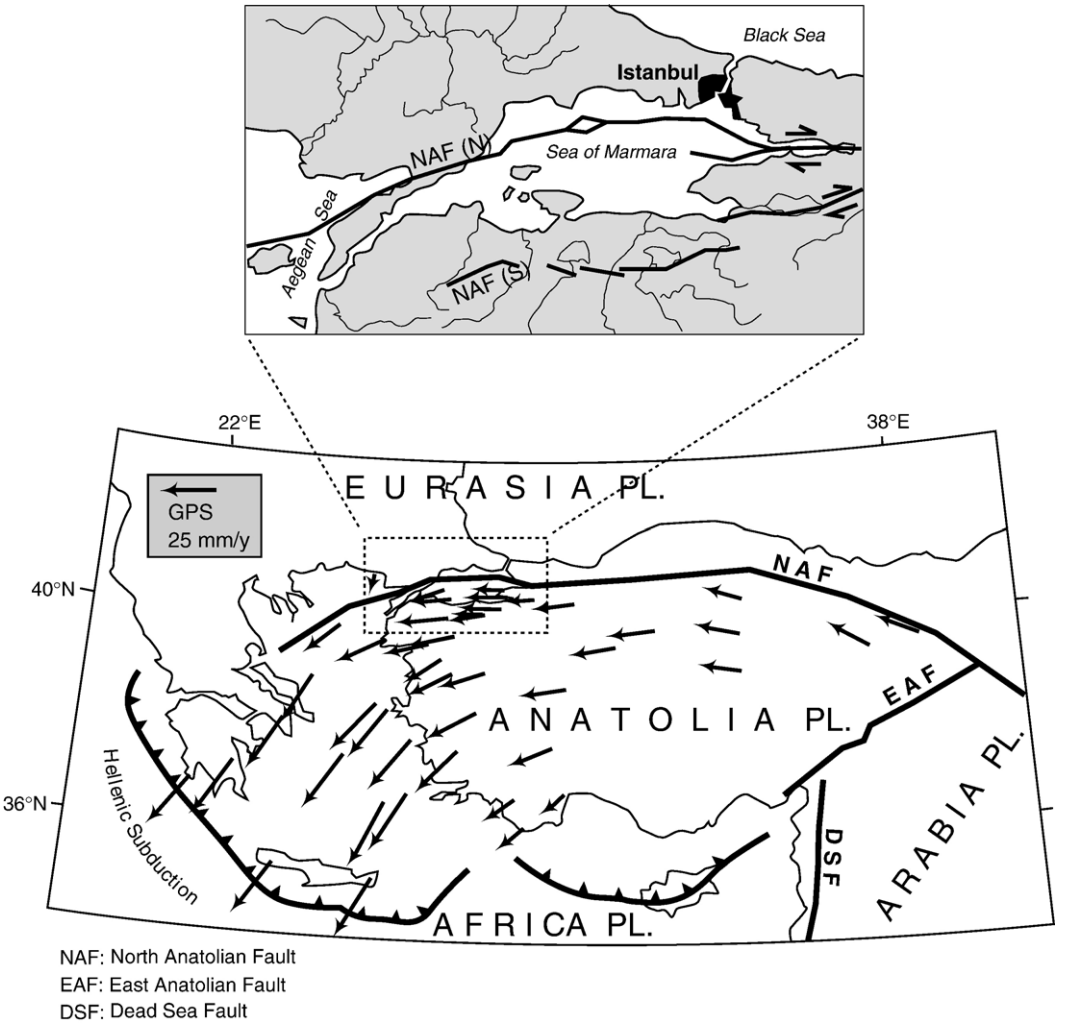

Fig. 1. Simplified present day geodynamic setting of the Sea of Marmara. (after Armijo et al., 1999, 2002); GPS velocity vectors with fixed Eurasia Plate, from McClusky et al. (2000). The Anatolia Plate is bounded by major strike-slip faults sytems (North and East) and subduction (South). The Sea of Marmara appears as a pull-apart basin created by right-lateral strike-slip displacement along the Northern Branch of the North-Anatolian Fault (NAF).

3. The Late Pleistocene–Holocene sedimentary fill of the Sea of Marmara: overview of MARMACORE Cruise's results

3.1. Technical aspects

The MARMACORE Cruise took place 20 August 13 September 2001, as part of the larger GEOSCIENCES MD 123 program. Onboard R/V MARION-DUFRESNE, a set of 8 long piston cores were retrieved using the CALYPSO piston corer. This retrieves up to 55-m long and 10-cm diameter cores. Five cores were taken at depths of 1250 and 1100 m, and three at shallower depths between 800 and 400 m. Lengths range from 21.8 to 37.3 m. Very high resolution single channel seismic reflection surveys were performed for site-surveying. In 2002, a grid of 3.5 kHz profiles were acquired during the MARMARASCARPS cruise, in addition to short piston cores (see Armijo et al., 2003); the whole dataset is located on Fig. 2. The eight long cores (labelled MD01-2424 to MD01-2432) were divided into 1.5-m long sections; non-destructive measurement profiles were performed, including Magnetic Susceptibility, sonic velocity, gamma-ray densimetry, using I.P.E.V.'s GEOTEK multitools core logger. Core sections were then split for visual description (layering type, sedimentary and tectonic structures) and preliminary sampling (smear slides for terrigenous and biogenic content analyses, plant debris and wood fragments for ^{14}C dating). Specific attention was paid to coarse terrigenous layers, microtectonic structures, and possible liquefaction features.

Preliminary shipboard studies were completed onshore by detailed Magnetic Susceptibility profiles using a BARTINGTON™ MS2 contact sensor (with 5 mm intervals). Laser microgranulometric measurements were performed using MALVERN™ Mastersizer S equipment. X-ray radiograms of split cores (MD01-2429 and MD01-2431) have been made with D.G.O.'s SCOPIX system (University of Bordeaux I); X-ray tomograms (in I.F.P. laboratory) have been performed on a selected portion of microfractured sediments in core MD01-2431.

3.2. Sediment compositions and types of layering

All analyzed sections (230 m in total) are basically composed of fine-grained terrigenous material with interlayered, sharply different, sequences that will be detailed here-after. The upper, marine, parts of the eight cores (see Fig. 3), are almost entirely composed of faintly-layered clayey-silty, slightly calcareous mud. Mean grain size, median, and mode, range between 4 and 8 μm, and calcite content is rather constant, around 15%. Detrital carbonate grains are generally dominant compared to bio-induced or biogenic components. These fine-grained sediments – "background" – are locally enriched in freshwater Diatoms frustules in the lower part; in the upper part, dispersed calcareous nannoplankton is present. In cores MD01-2425 and MD01-2427, we observed a conspicuous millimetric layer consisting of an almost pure nannoplankton ooze (Fig. 3); we tentatively used this "bloom" as a correlation chronological marker. The silty terrigenous fraction is siliciclastic, mainly of volcanogenic origin (fresh plagioclase, amphibole and pyroxene, fresh automorphous brown mica, opaques minerals); metamorphic and plutonic rocks-derived components (white micas, amphiboles, deformed quartz) are rare. More frequently in the lower part, dark pigmentation is developed, due to diagenetic sulfides; either diffused or concentrated in association with bioturbation.

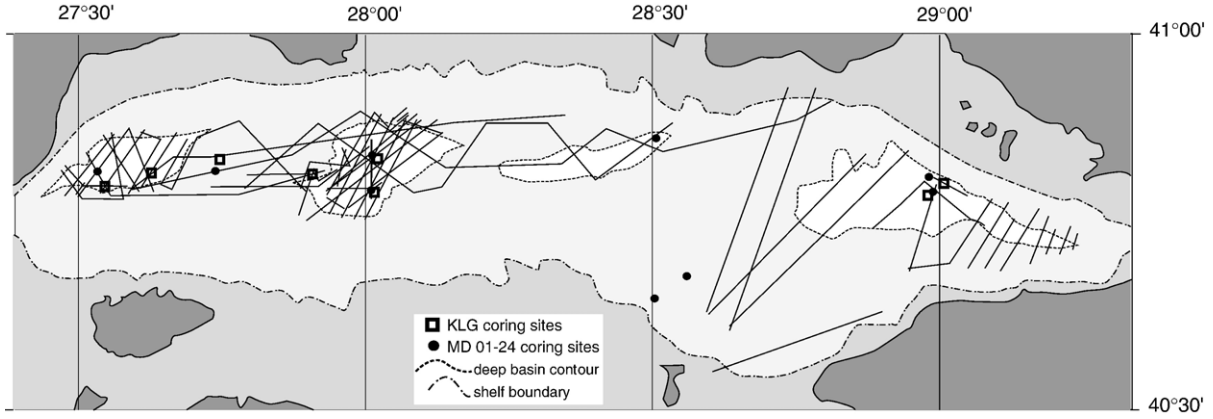

Fig. 2. High resolution seismic reflection grid and coring locations of MARMACORE and MARMARASCARPS Cruises.

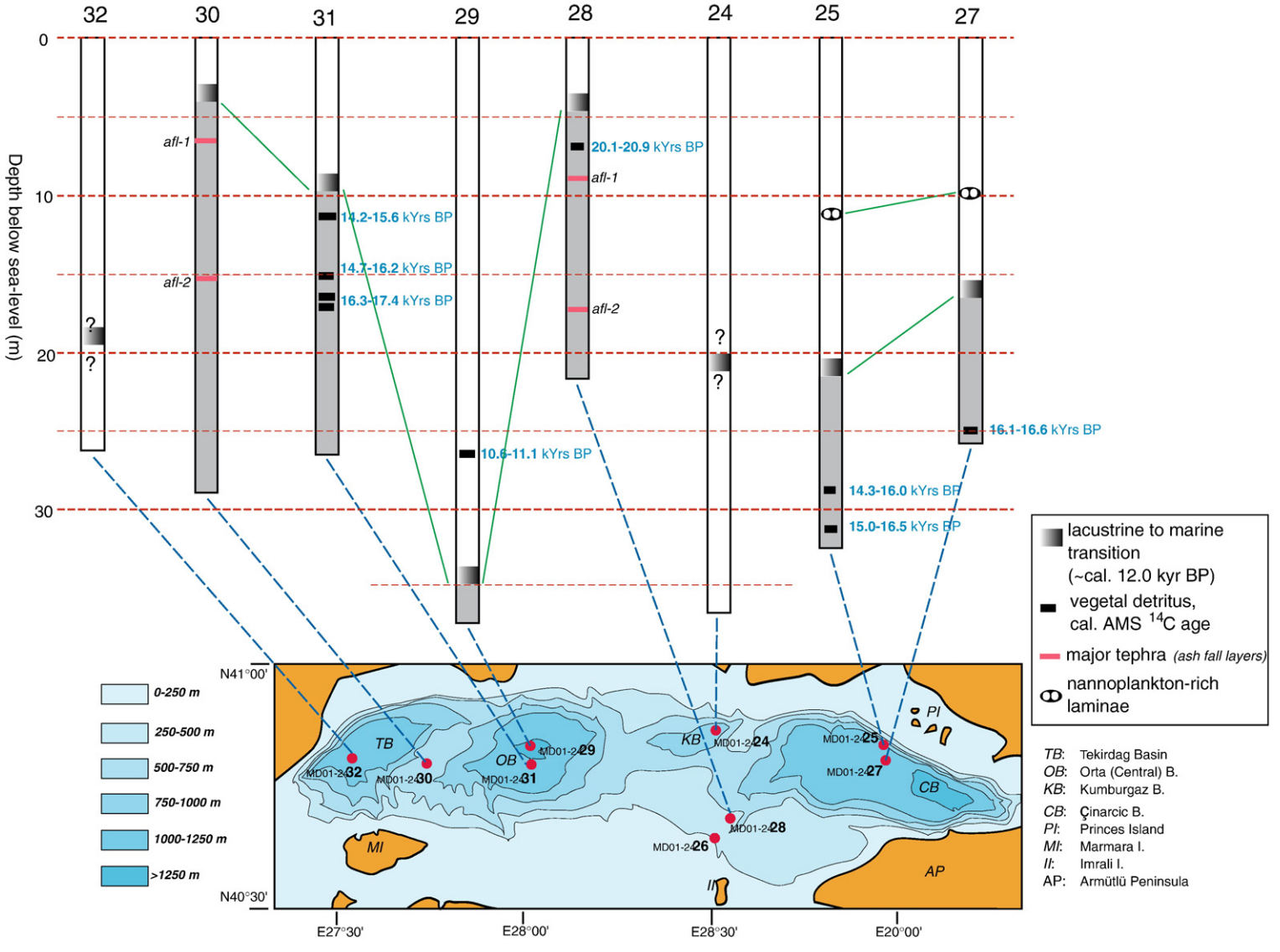

Fig. 3. Summary of giant piston coring results in the Sea of Marmara (MARMACORE Cruise), and shipboard proposed lateral correlations.

Noteworthy individual layers (events) or successions of layers are intercalated within the background clayey-silty (marine or lacustrine) sediment:

- ash layers: Two major probable pyroclastic fallout events, up to 8-cm thick, have been found in cores MD01-2428 and MD01-2430 and tentatively correlated (afl-1 and afl-2; Fig. 3). These two sites show a sedimentation rate much lower than in other cored sites. Several discrete (less than 5-mm thick) ash-enriched layers are present in all cores;
- silty-sandy laminated intervals: these are abundant in lower half of the marine interval of cores MD01-2424, MD01-2425, MD01-2427 (eastern basins), and more dispersed in core MD01-2432 (western basin). In cores MD01-2429 and MD01-2431 (Central Basin), these intervals are intercalated within the upper marine sequence. They consist of millimetric parallel planar bedding, involving subtle changes in grain size and mineralogy of detrital components. According to textures and composition, we interpret this layering as related to bottom horizontal bed-load distribution. It does not represent fluctuations in planctonic production and/or in parapelagic suspended load. The apparent cyclic layering could represent variations in locally developed bottom currents as responses to surface ones, in a convective-like system; this possible process could be more active close to the two sills. An alternative explanation may be that these coarser laminated episodes represent distal distribution of flood-induced dense bottom currents, and, thus, periods of particularly strong and repeated runoff (?). These two speculative interpretations converge to a paleoenvironmental forcing; they need further detailed laboratory analysis;
- turbiditic sequences: These are common in the deepest cores (MD01-2424, MD01-2425, MD01-2427, MD01-2429, MD01-2431) except for the Tekirdag Basin. Ranging from centimetric to decimetric thickness, they are almost entirely intercalated within the lower, lacustrine, part of the analyzed successions. We observed the apparent highest frequency in Central Basin's core MD01-2431. These turbidites usually display a sharp erosive base, sometimes with ball-and-pillow structures; the basal coarse sands contain shell fragment concentrations, and sometimes plant detritus. The mineralogy of the siliciclastic fraction is similar to the one observed in the finer-grained strata mentioned above. Part of these turbidites show a classical progressive fining upwards, while, for the thickest ones, an abrupt contact separates the bed-load basal part from the suspended-load upper part, the latter turning into a "homogenite". One of the following paragraphs will focus on these specific sedimentary "events", and especially on an 8-to-12-m thick sequence which itself comprises a 5-to-8-m thick homogenite.

Table 1
A.M.S. Radiocarbon dating results from organic debris

Sample	Type	δ13C	Age	Age error	Calibrated age BP, 95.4% conf.
MD012425–2816 cm	Plant/Wood	−26.81	12850	55	15 950/14 350 yr
MD012425–3105 cm	Plant/Wood	−26.66	13250	55	16 450/14 950 yr
MD012427–2498 cm	Charcoal	−27.82	13600	55	16 850/15 800 yr
MD012428–696 cm	Charcoal	−28.83	17200	70	21 150/19 750 yr
MD012429–2705 cm	Charcoal	−26.45	9530	45	11 100/10 920 yr (44.7%) 10 910/10 670 yr (49.5%) 10 660/10 640 yr (1.2%)
MD012431–1138 cm	Charcoal	−28.12	12150	65	15 650/14 250 yr
MD012431–1518 cm	Plant/Wood	−27.86	13100	55	16 250/14 750 yr
MD012431–1661 cm	Plant/Wood	−28.74	14100	75	17 450/16 350 yr

Analysis performed at Woods Hole Oceanographic Institution, National Ocean Sciences Accelerator Mass Spectrometry facility (NOSAMS); calibration with OxCal Program v3.10.

Both within the marine and the lacustrine parts of the cored succession, bioturbation appears very scarce; black sulphidic lenses may represent millimetric simple burrows. As observed in deep lacustrine basins or in isolated marine basins, this suggests anaerobic to dysaerobic conditions. The occurrence of a few bioturbated horizons at the top of turbidites/homogenites underlines possible reoxygenation related to episodic bottom currents initiated in shallower oxygenated areas.

3.3. Chronology and correlation with data from shelves

Shipboard preliminary lithostratigraphic correlations (Mercier de Lépinay et al., 2001) were based on a few conspicuous layers (major tephra and nannoplankton "blooms"). More detailed observations of biogenic content distinguished the marine upper part from the lacustrine lower sediments, thus completing the correlation chart.

Ten plant/wood or charcoal fragments and two mollusc shells were found during shipboard core-splitting. They

were used for A.M.S. ^{14}C analyses performed at Woods Hole Oceanographic Institution, National Ocean Sciences Accelerator Mass Spectrometry facility (NOSAMS) (11 samples), and in Zürich Federal Polytechnical Institute (1 sample). Only results concerning organic matter samples (Table 1) are indicated on Fig. 3 and used in our discussion. Raw values were calibrated according to the variations of atmospheric ^{14}C (Stuiver et al., 1998). We used OxCal Program v3.1. Values plotted on Fig. 3 logs correspond to highest confidence intervals. Most of the cores appear to represent the Holocene and part of the Late Pleistocene. The longest core (MD01-2429, 37.3 m), represents the shortest time interval sampled, and was retrieved from the deepest zone of the Central Basin. Conversely, cores MD01-2428 and MD01-2430 may represent the last 40 to 50 kyr BP, if mean sedimentation rates extrapolated.

Our chronological data are in agreement with the lacustrine-to-marine transition age proposed by various authors: around 12 cal. kyr BP (Çağatay et al., 2000; Tolun et al., 2002; Çağatay et al., 2003). Due to the importance of the "corridor" situation of the Sea of Marmara, between the Black Sea and the Aegean, the Late Quaternary connection has been investigated and discussed by various authors, based on coring results and high resolution seismic reflection data, (Aksu et al., 2002a,b; Major et al., 2002; Hiscott and Aksu, 2002). Our preliminary results are in agreement with chronological data from shallow sedimentary records (southern shelf and Izmit Gulf) (Çağatay et al., 2000, 2003); we did not observe any abrupt change, favouring the "deep sill" rather than the "shallow sill" models of Major et al. (2002).

For cores MD01-2429 and MD01-2431, we reconstructed two synthetic logs with potentially reflecting interfaces, based on detailed layering and sediment texture contrasts. These logs were then compared to corresponding portions of 3.5 kHz seismic lines, taking into account an estimation of theoretical vertical resolution (Fig. 4). In the upper marine part, the "background" sedimentation is slightly variable with a high siliclastic (clay–silt) and calcareous fraction, and is

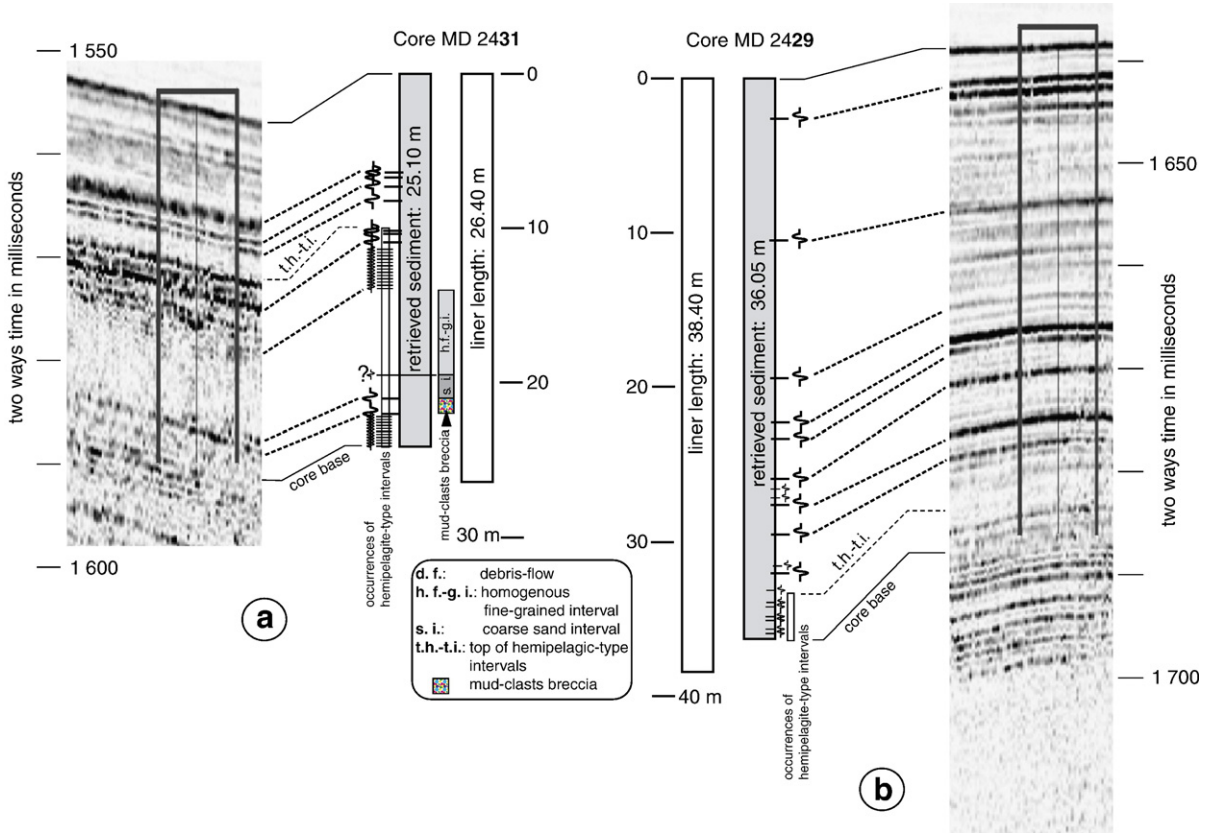

Fig. 4. Synthetic seismic logs of cores MD01-2429 (b) and MD01-2431 (a): location of main potential reflective sedimentary interfaces (left) and correlation with detected reflectors (right). The marine upper part corresponds to variable amplitude and variable frequency; the lacustrine "hemipelagic-type" lower part corresponds to almost constant amplitude and high frequency.

interrupted by only a few coarse turbiditic layers. The last mentioned are correlated with a few high amplitude reflectors (see Fig. 4b, 0–32-m interval of core MD01-2429 and corresponding acoustic image; 1640–1685 m t.w.t.). Other reflections have variable amplitude and variable frequency. In the lower part, the "background" sedimentation is finer-grained and with a more constant composition (dominantly biogenic and bio-induced material). This "hemipelagic-type" sediment often appears as clear thin intervals (few cm to 10 cm; close-ups of Fig. 5) between numerous coarse turbiditic layers. As they are intercalated within more constant background sediment, they produce constant amplitude and high frequency reflections (see Fig. 4b, interval below 32 m in core MD01-2429 and corresponding acoustic image below 1685 m t.w.t.). Thus, the separation of the

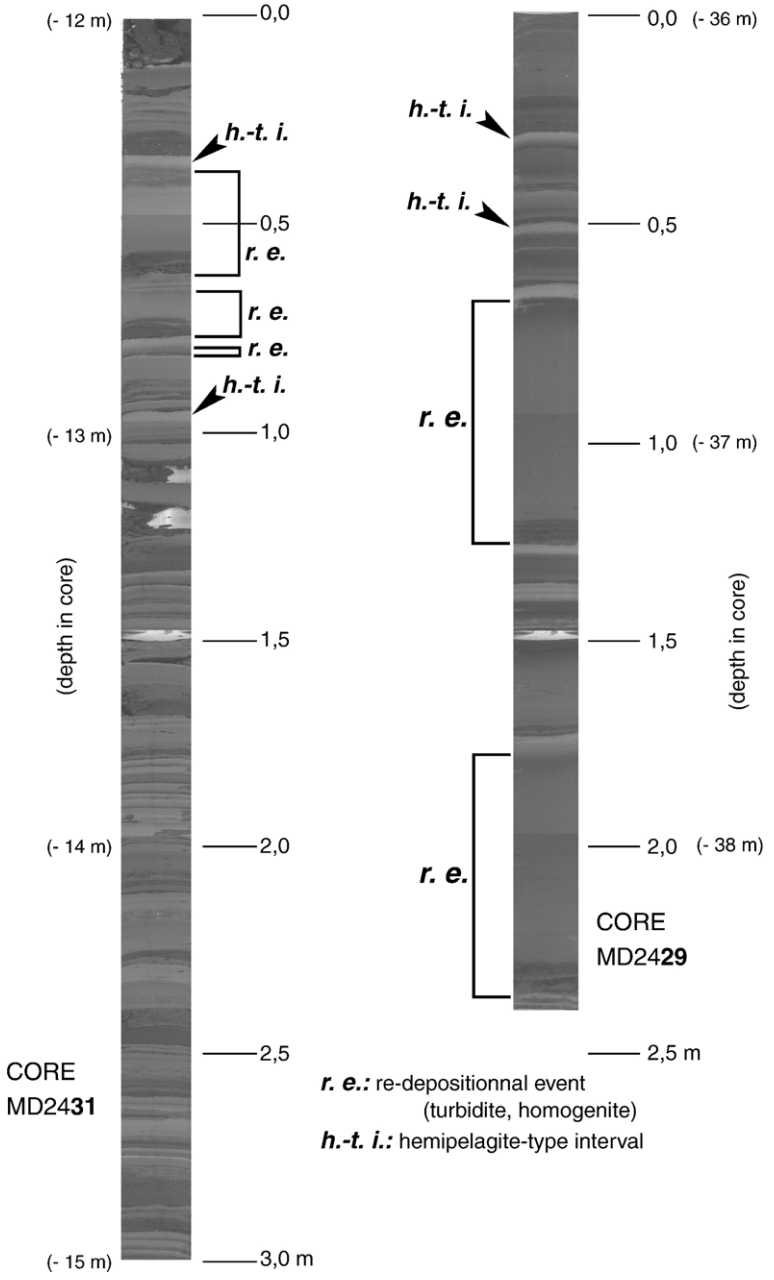

Fig. 5. Close-ups of split sections of the lower lacustrine part of cores MD01-2429 and MD01-2431, displaying the frequency of strong contrast interfaces between the "hemipelagic-type" background sediment and coarse re-depositional events.

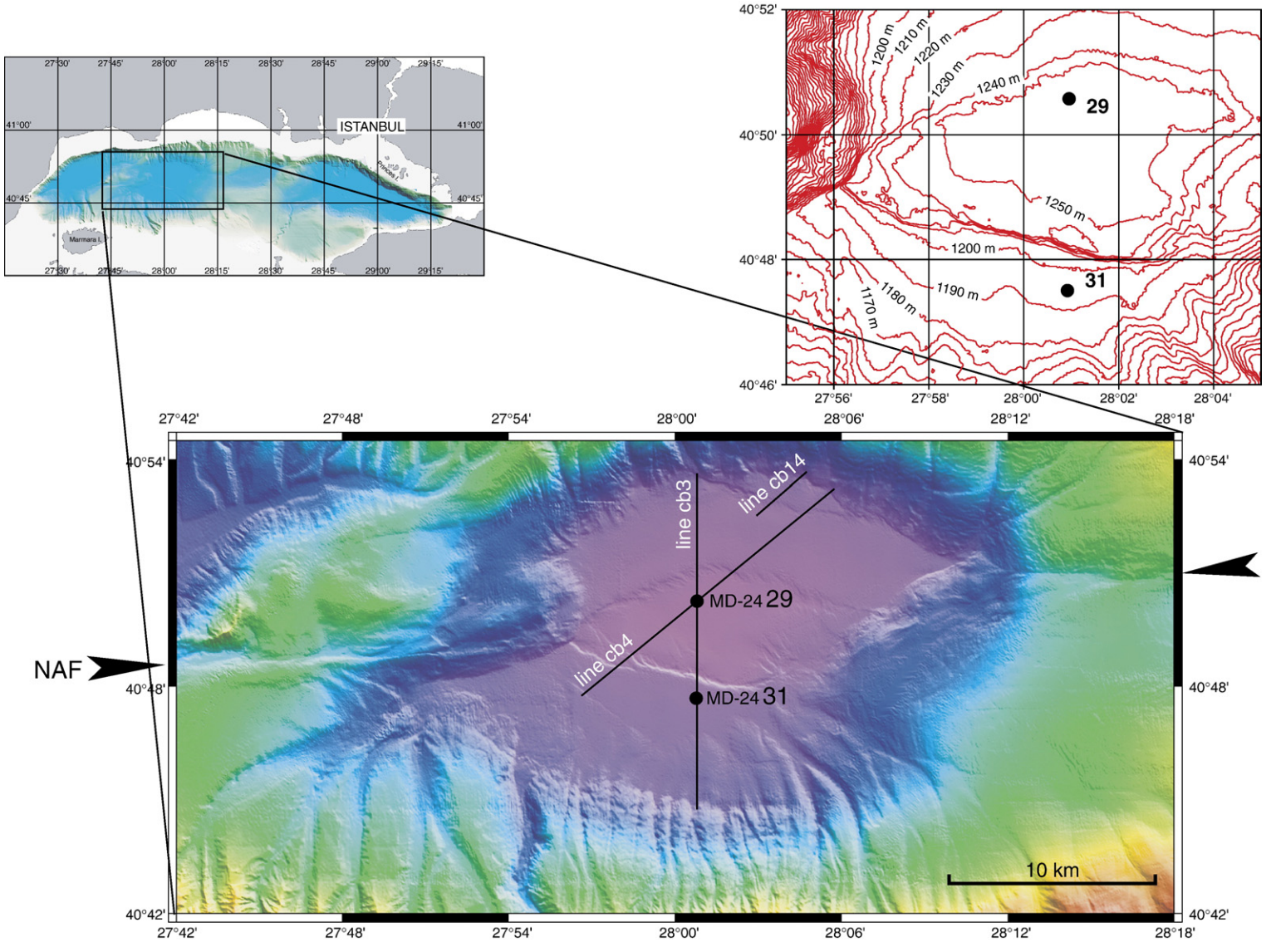

Fig. 6. Detailed morpho-bathymetry of the Marmara Sea's Central Basin, location of giant piston cores and seismic profiles.

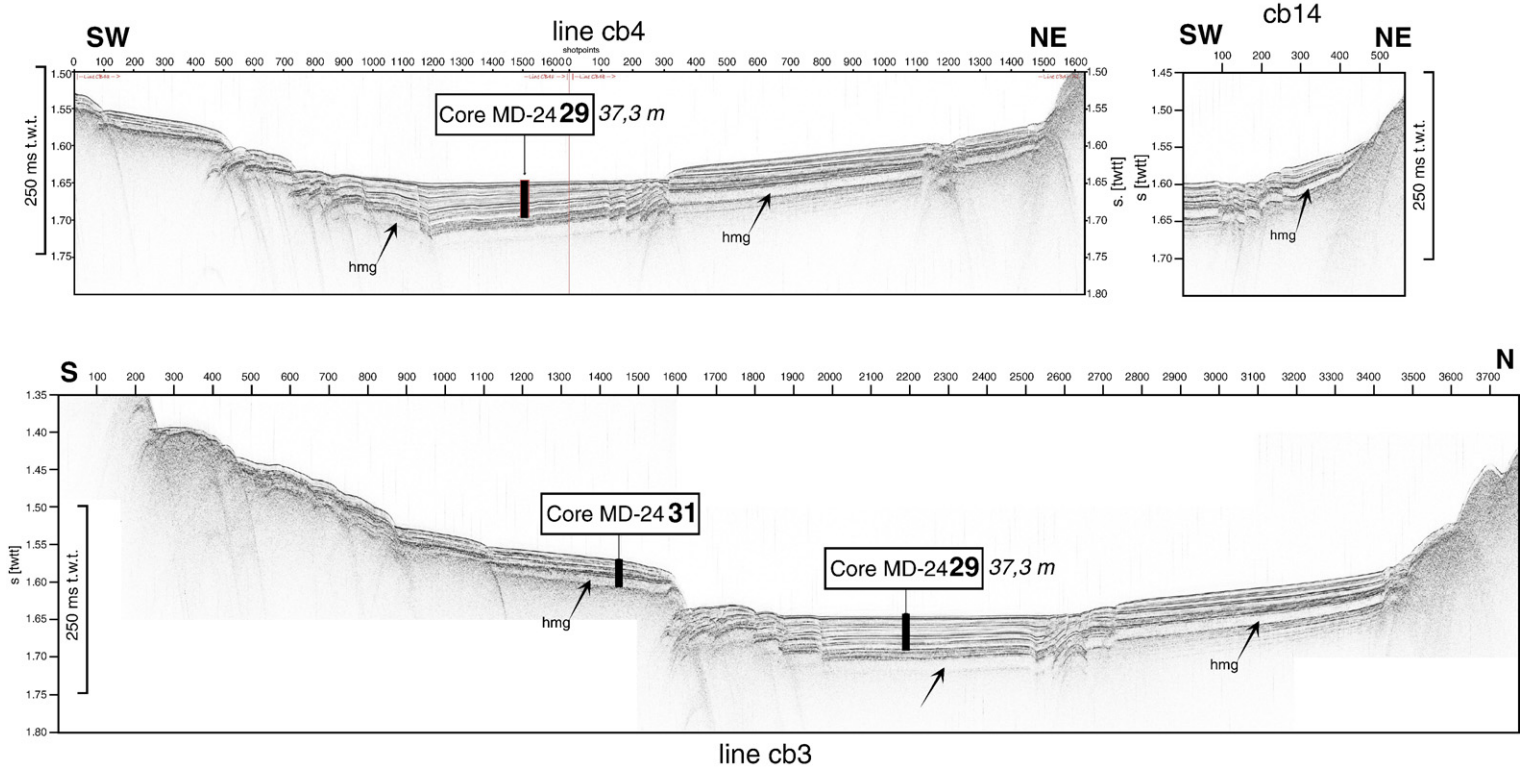

Fig. 7. 3.5 kHz profiles across the Central Basin, showing evidence for an “homogenite”.

upper marine period of sedimentation from the lower lacustrine (hemipelagic-type) can also be traced on the high resolution seismic imagery. For the two studied sites at least, this limit is consistent with other previously mentioned data. On Core MD01-2431 (Fig. 4a), the characterisation of the lower "hemipelagic-type" interval

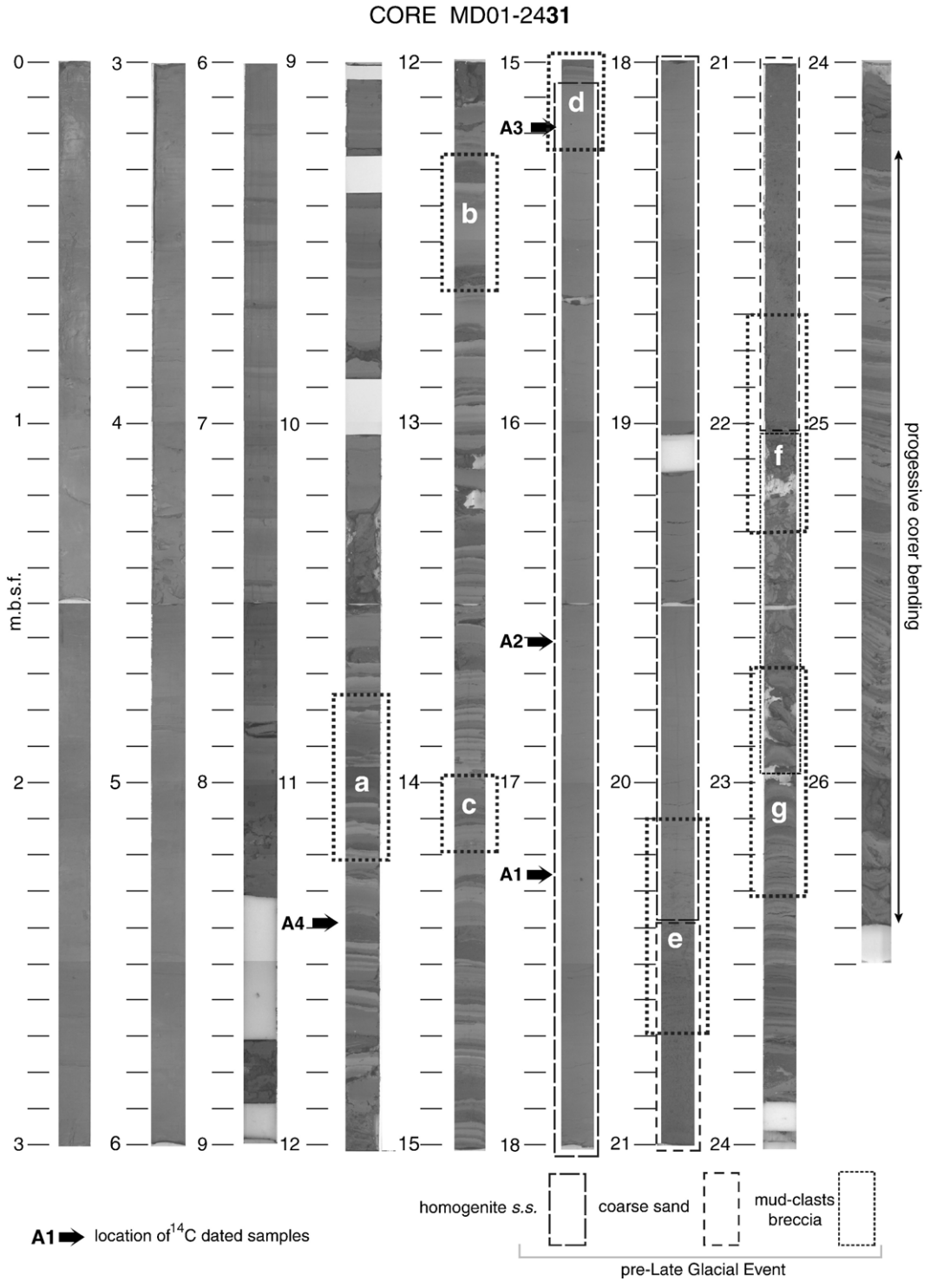

Fig. 8. General view of split core MD01-2431, showing the pre-Late Glacial "homogenite" and associated coarse gravity deposits.

is not so obvious due to the presence of the 8-m-thick megaturbidite described in the next paragraph.

3.4. Occurrence of a major pre-Late Glacial sedimentary "event" in the Central Basin

The various seismic profiles crossing the Central Basin (Fig. 2) display a conspicuous acoustically transparent layer up to 8 m two-way-time in thickness. Taking into account the theoretical vertical resolution, analysis of the complete grid did not allow clear identification of this layer in the other sub-basins (Tekirdağ, Kumburgaz, Çinarcic). Nevertheless, the chronostratigraphic resolution of the cores indicates the presence of a more subtle signature of the same sedimentary "event", as one of the re-depositional event features on Fig. 5. This homogeneous layer, term on "homogenite" in reference to the concept of Kastens and

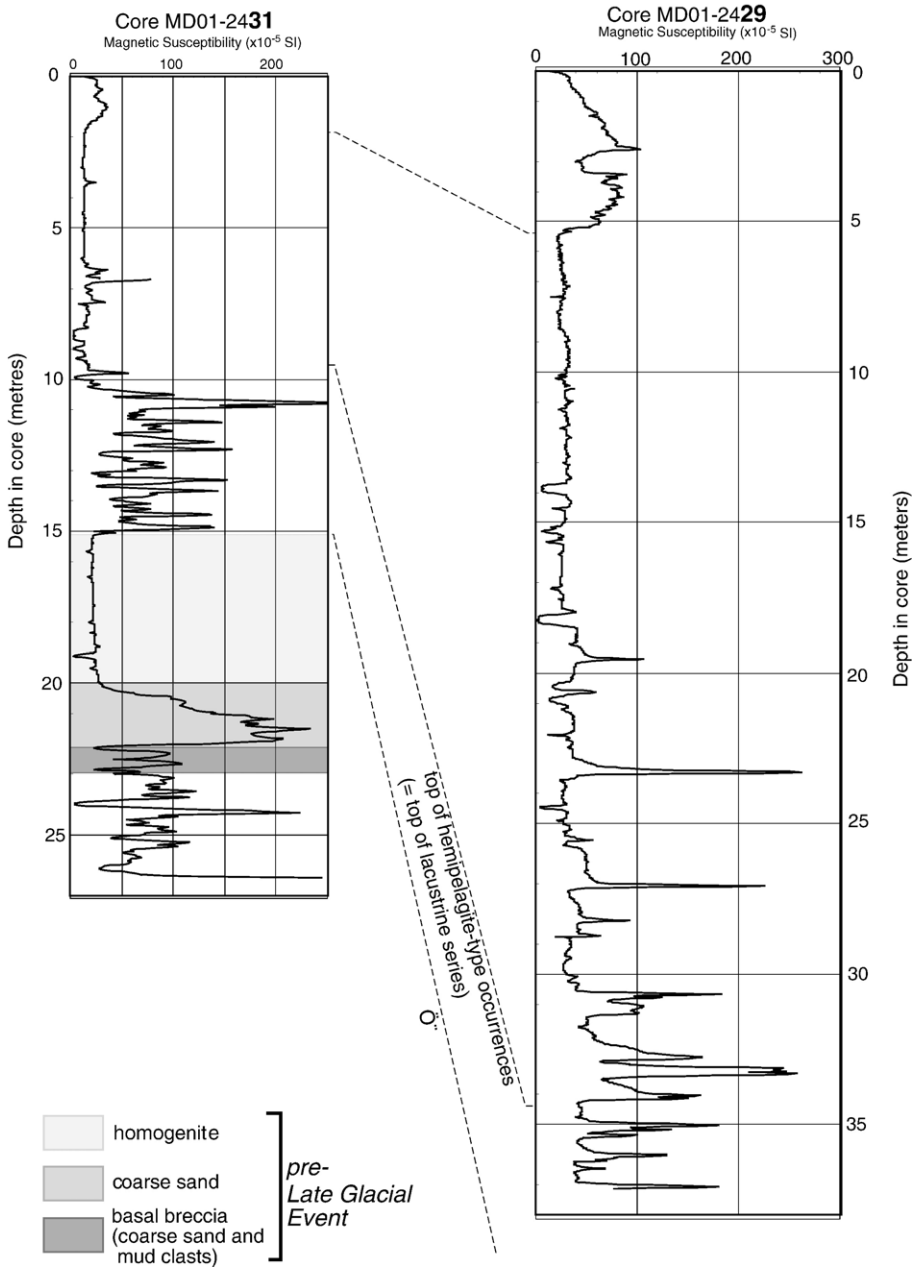

Fig. 9. Correlations between cores MD01-2431 and MD01-2429 based on Magnetic Susceptibility.

Cita (1981), will be emphasized as the upper component of a unique huge re-depositional event.

3.4.1. Ocurrence of a pre-Late Glacial homogenite

Fig. 7 profiles (location on Fig. 6) underlined a specific distribution of the homogeneous transparent acoustic layer, and its characteristics, namely

- restriction to the very deepest parts of the Central Basin (below 1190-m depth),
- sharp lateral termination (see line cb 14, Fig. 7),
- increasing thickness with increasing depth (comparison of central and western parts of line cb3, Fig. 7).

The "homogenite" represents very fine-grained sediment likely transported and deposited as suspended load. The lack of vertical changes and the non-draped configuration implies deep horizontal spreading, similar to any hyperpycnal depositional process. Based on the whole grid of chirp profiles of the Central Basin, the total volume is estimated at between 0.6 and 1.4 km^3.

Core MD01-2431 completely crossed this homogeneous layer; it can be viewed on a general reconstructed picture (Fig. 8). Within the uppermost 70 cm, three dispersed wood fragments were extracted. Calibrated ages with maximum confidence intervals are: 16.6–17.3 cal. kyr BP for samples A1 and A2, 15.5–16.0 cal. kyr BP for sample A3. Considering the wood debris as reworked, we selected the youngest age as the closest to the homogenite deposition age, assuming a unique event as argued below. About 2 m higher in a layered part of core MD01-2431, another wood fragment yielded a 14.1–14.8 cal. kyr BP age (sample A4). This is in agreement both with the age proposed for the homogenite, and the age of the lacustrine-to-marine transition detected above. In the following, we will name this unit the pre-Late Glacial homogenite (PLGH).

3.4.2. Association of the pre-Late Glacial Homogenite with a coarse-sand and mud-clast layer

Between the PLGH and the next underlying "background" hemipelagic-type layer, two thick and coarse layers are intercalated (Fig. 8):

1) 1.7 m of dark siliciclastic non-stratified coarse sand, with minor biogenic content from a shallow coastal environment (highly fragmented molluscs shells), and dispersed millimetric plant debris;
2) 1.0 m of mud–clast breccia; its centimetric clasts are made of fine-grained grey to whitish sediment, with locally preserved stratification; they are embedded within a coarse sand matrix identical to the overlying one. Based on microscopic observation of terrigenous and biogenic fractions, the mud clasts are interpreted as reworked from the underlying well-stratified lacustrine sequence.

The Magnetic Susceptibility (M.S.) signature of these two coarse layers (Fig. 9, left graph) reinforces the distinctiveness of the coarse sand and the similarity between the mud clasts and the underlying succession. The M.S. of the homogenite is also remarkably constant. The upper marine sequence also yielded, between 2 m and 6 m, a rather constant M.S. profile but with a different (lower) mean value. The homogenite's carbonate content is nearly constant, between 12.9 and 13.1%.

Detailed grain-size vertical evolution profiles (Fig. 10) are based on regular sampling of the homogenite and coarse sand layers. All parameters (mean grain size, mode, median: between 6 and 7 μm) are highly constant in the homogenite, and more varied in the coarse sand. Part of the results is plotted as a base-to-top path on a skewness *vs.* sorting diagram (Fig. 10), which shows or confirms:

1) fluctuations of depositional dynamics in the bed-load part, the displayed variation frequency being probably higher than the one detectable by the sampling interval;

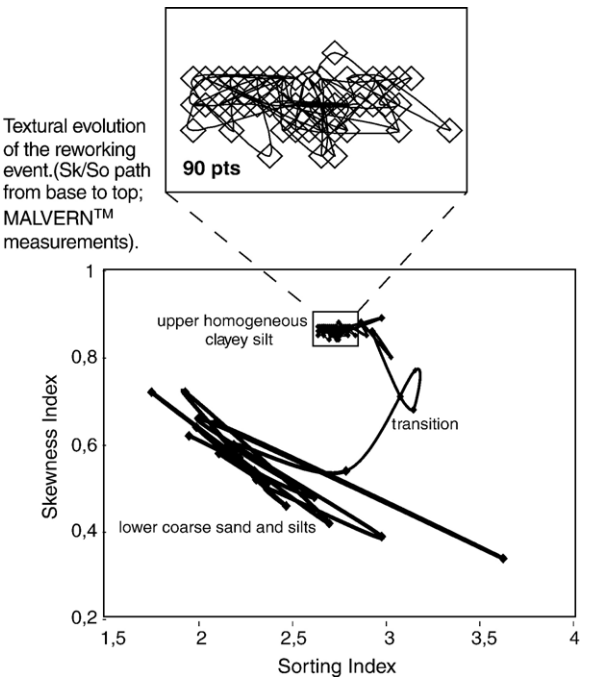

Fig. 10. Vertical evolution of grain-size distribution in the pre-Late Glacial Event.

2) sharp transition between the coarse sand and the homogenite;
3) highly constant distribution along the 5-m thickness of upper, suspended load, part.

The three layers are considered to be components of a unique re-depositional "event", totaling 8-m thickness in core MD01-2431: the pre-Late Glacial Event (PLGE).

Close-ups in Fig. 11 illustrate different parts of the PLGE: the top, with transition from homogenite to hemipelagic-type sediment (Fig. 11d), the coarse sand/homogenite boundary (Fig. 11e), the mud-clast interval/coarse sand boundary (Fig. 11f), and the base of the mud-clast interval (Fig. 11g). Except for the last mentioned, the whole set is composed of allochtonous siliclastic components derived from previously deposited shallower (shelf and shelf margin) sediments. The diatom assemblages determined within the sand, the mud-clast breccia, and the homogenite (Boutareaud, 2003) belong to various mixed shelf and delta

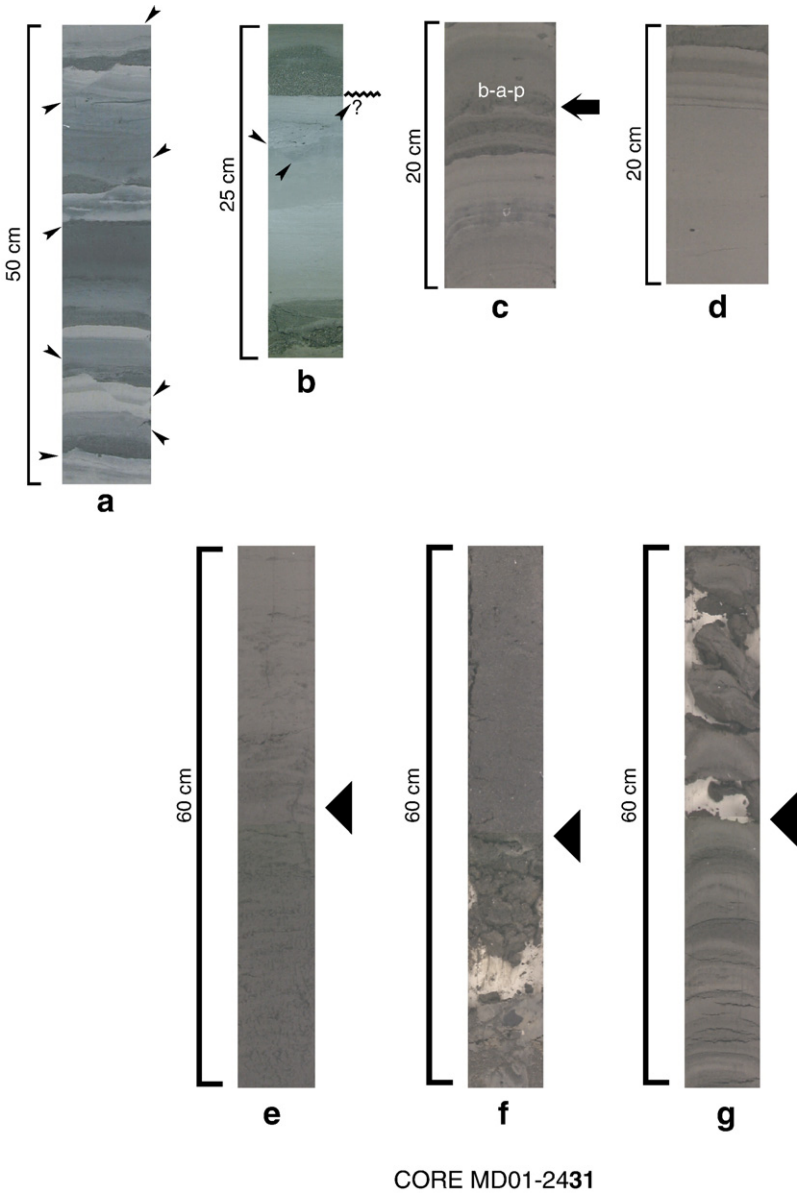

Fig. 11. Close-ups of selected portions of core MD01-2431. (cf. Fig. 8; a: conjugate microfractures; b: microfracturing with possible sealing by coeval turbidite arrival; c; possible *in situ* liquefaction, evidenced by ball-and-pillow – b-a-p – structure; d to g: details of the pre-Late Glacial event. In the continuous core section from 10.50 m to 12.00 m X-ray scanning show a constant orientation of microfractures).

environments. This confirms the reworked origin and especially argues against a unique "hemipelagic" source for the homogeneous upper layer.

3.4.3. Depositional model for the pre-Late Glacial event and smaller-sized similar events

Generally speaking, the depositional model proposed for the PLGE follows the concept of a megaturbidite: large volume mass wasting turning into a dense hyperpycnal flow (Bowen et al., 1984; Mulder et al., 1994; Mulder and Cochonat, 1996; Bouma, 2000). Nevertheless, the distinct boundary between the coarse sand and the upper fine-grained unit and the lack of clear internal structures differ from the usual configuration of classical turbiditic sequences. This sharp boundary is also common on smaller-sized sedimentary "events" (Fig. 5). The Mediterranean "Minoan" homogenite (Kastens and Cita, 1981; Cita et al., 1996) is not associated with a coarse base layer, and units of these type were called "unifites" (Stanley, 1981; Stanley and Maldonado, 1981). Also, Stow and Wetzel (1990) proposed the "hemiturbidite" concept for fine-grained homogeneous layers, explained by a deep-seated separation of an upper fine-grained "cloud" from a lower coarser-grained layer, the former following a much longer trajectory. This separation may also be explained by a "hydraulic jump" (Fig. 12, case a). This concept explains the horizontal separation, within a unique mixed particulate flow, of an upper suspended-load flood from a (coarse-grained) basal, quickly immobilized, layer. This separation is attributed to bottom relief acting as an obstacle. Initially proposed for

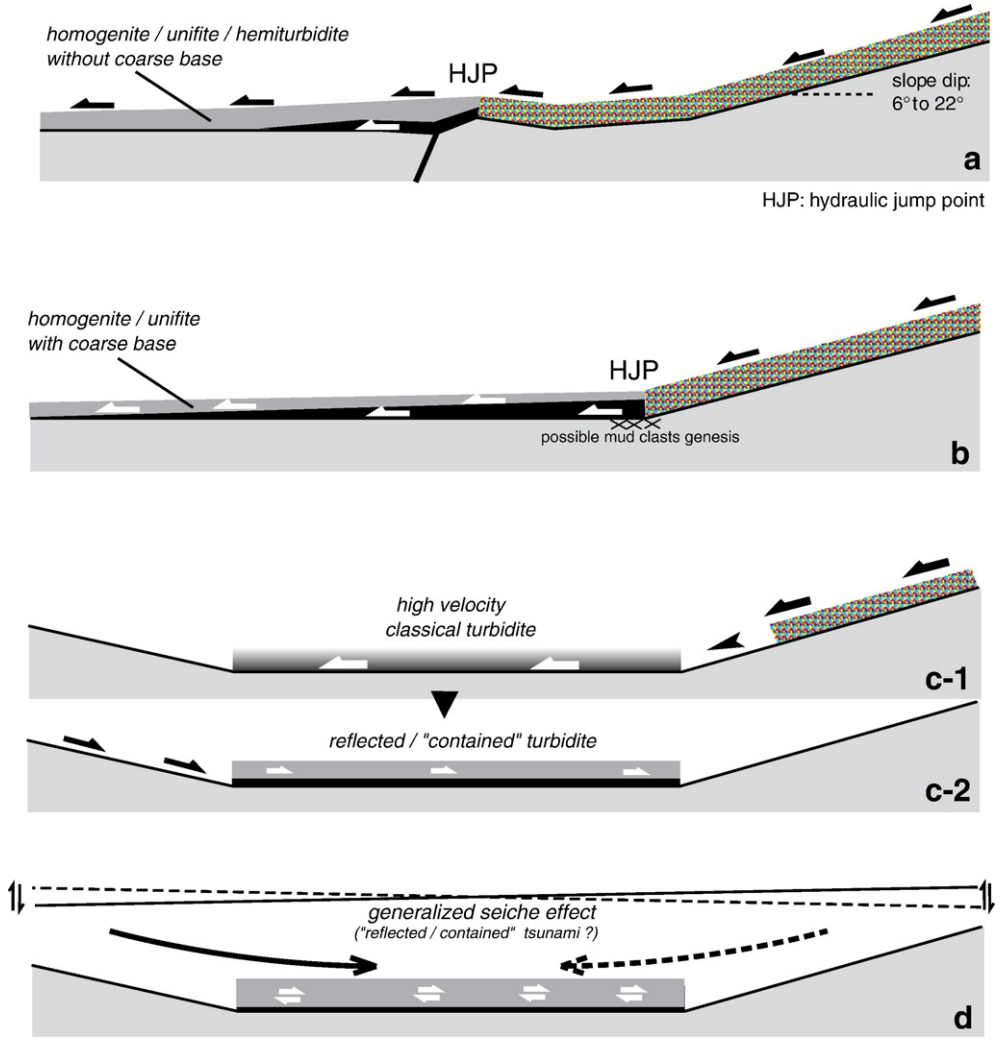

Fig. 12. Different explanatory models for the segregation of homogenite layers.

coastal sediments, the hydraulic jump concept has been applied to deeper situations as deltaic foresets and turbidites (Komar, 1971; Nemec, 1990; Kubo and Yokokawa, 2001; Allen, 2001) without necessarily implying an obstacle. In a turbidity current, the separation (jump) may occur while crossing the slope (within the canyon), or at the deep plain/slope break (Fig. 12, case b).

Nevertheless, for the PLGE and for smaller-sized similar sedimentary "events" (Fig. 5), the coarse basal layers are present and are supposed to have spread horizontally together with the upper fine-grained suspension. Furthermore, the 3.5 kHz profiles show the same "acoustic" structure (and thus same composition) for the PLGE throughout the Central Basin. The 3.5 kHz profiles do not show any major relief below the PLGE, but rather a flat surface that pre-dates the youngest fault scarps.

As an alternative explanation we propose a long-lasting bottom current with several superimposed direction changes, leading into an almost complete segregation of the bedload from the suspended load (Fig. 11). This could be induced by:

1) either a high velocity turbidity current (high kinetic energy) undergoing several reflections against the steep slopes of the Central Basin with progressive damping (following the concept of "contained turbidites" of Pickering and Hiscott, 1985) (Fig. 12, case C); or
2) an oscillatory movement of the whole water mass, initiated by a sudden bottom modification (co-seismic displacement, or huge sub-aqueous slump) (Fig. 12, case D). This tsunami effect has been analyzed and modelled for the Sea of Marmara (Yalçiner et al., 2002); it also can be considered as a seiche effect as known in large lakes (Siegenthaler et al., 1987; Chapron et al., 1999). The second hypothesis is directly "paleoseismic", and the first mechanism proposed is also often considered as earthquake-triggered (Nakajima and Kanai, 2000). We assume (see also Chapron et al., 1999; Beck, in press) that this oscillatory mechanism is responsible for:
   a) additional extraction of clayey-silty matrix from the initial flux, leading to an increased volume of upper suspended load, and sharpening the boundary between coarse and fine-grained layers;
   b) concentration (ponding) of the homogenite deposit within deepest hollows.

In contrast, in a single fine-grained turbidite flooding a wide basin floor, the widespread and thick upper suspended "cloud" may partly lead to upslope deposition with local draped configuration (Dolan et al., 1989).

We do not have any direct evidence (on HR seismic images) for corresponding slump scars, and have to consider two alternate origins: a unique major mass wasting, or the gathering of several slumps turning into coeval turbidites channelized by the different canyons of the southern edge of Central Basin (Fig. 6). Two departure areas could be proposed: the edge of the main large shallow southern shelf or the deeper irregular inclined shelf mainly bounding the eastern half of the Sea of Marmara (North of Imrali Island, see Fig. 3). We favour the first hypothesis because: 1) following the present day subaquatic morphology, the Central Basin is not directly affected by the drainage crossing the deep eastern shelf; 2) the less steep slope was well imaged by HR seismic and no slump scar was detected.

The presence of mud clasts of deep autochthonous origin, reworked at the base of the PLGE megaturbidite, needs an additional specific mechanism. We propose two explanations: either they are generated within the megaturbidite along the slope–bottom break line (Fig. 12, case b), or they are a direct consequence of a major earthquake inducing submarine scarps and microfaults (Fig. 13). In the second hypothesis, the megaturbidite is generated by the same shock and may be called seismoturbidite.

Taking in account the various available data previously mentioned, we favour, for this huge pre-Late Glacial Event, the combination of a major earthquake (16,000 cal. yr BP) occurring during a period of high terrigenous sedimentary supply related to specific Late Glacial climatic conditions. With respect to smaller-sized reworking events (Fig. 5), they are believed to represent similar mechanisms, with similar triggering, and in a similar situation with respect to climatic fluctuations. In several cases, these turbiditic layers appear as "sealing" previous disturbances of the underlying sediment/water interface (Fig. 11, close up b); the volume differences (or thickness differences) between all these sedimentary events, must be related to a combination of: 1) the characteristics of the triggering shaking (unique short event *vs*. repeated shocks); 2) the type of impact on sedimentation (number of induced mass wastings, size of slope failure, intensity of direct bottom disturbance (Rodriguez-Pascua et al., 2002), 3) the distance between the investigated depositional basin and epicentral area (Lignier, 2001).

All these sedimentary "events" have been investigated in the lacustrine lower part of the Central Basin's

recent fill as they are striking features. Does it mean that this process decreased or disappeared in the Holocene? Or did the earthquakes' sedimentary record become weak or absent? The following section deals with the impact of strong seismic activity during the marine (Holocene) sedimentation.

4. Overthickening of the sedimentary pile with increasing depth in the Central Basin

The general configuration of the Sea of Marmara's sedimentary fill, as imaged by seismic reflection (Okay et al., 2000; Rangin et al., 2001; Le Pichon et al., 2001; Ímren et al., 2001; Carton, 2003; Hirn et al., 2003; Demirbağ et al., 2003), clearly indicates a complete, long term, tectonic control of the sedimentary fill; especially for internal configurations in the different sub-basins. With the higher resolution here used, this relationship may be envisaged, not as a continuous process (with mean values of sedimentation rates and of fault displacements), but rather as a succession of incremental events (with instantaneous sedimentation rates and co-seismic faults scarps). Both on chirp profiles and in cores, this second investigation scale enables explanation of very local and large thickness increases such as the one observed in the Central Basin's deepest part (Fig. 7).

4.1. Correlation between cores MD-2431 and MD-2429

The synthetic seismic logs based on core lithological content, and constructed for general seismostratigraphy (Fig. 4), were used for detailed correlation across the deep fresh scarps zone subdividing the Central Basin floor (Fig. 7). The correlation between Cores MD01-2429 and MD01-2431 (Fig. 14), established with 3.5 kHz images, and completed by lithological comparisons, illustrates the differences. The horizontal distance is less than 10 km and the bottom depths are respectively about 1250 m and 1200 m. Assuming a constant mean sonic velocity in the imaged sedimentary pile, the upper marine part (above the "hemipelagite-type" occurrences) is three times thicker in Core MD01-2429 than its lateral time equivalent. The same increased rate may be measured deeper in the core, in strata overlying the PLGH. The "homogenite" itself shows a 75% thickness increase. Considering the detailed accumulation processes in the lacustrine part (see close-ups in Fig. 5), the slow "background" sedimentation represents 10 to 20% of the total rate in core MD01-2431 (upper part of left log on Fig. 5). In MD01-2429 (lower part of right log on Fig. 5) the sedimentary "events" representing instantaneous deposits (like the PLGE) are much thicker, and the "background" sedimentation represents less than 10% of the total rate. The "hemipelagic-type" thickness is almost the same in both cores, indicating negligible reworking of this material, taking account of either individual thickness or their total. The strong total thickness increase in the lacustrine part, between the two sites, is thus basically due to the addition to the thickness differences arising from each individual gravity "event". According to the sedimentological interpretation proposed above (Section 3.4.3), the differences across the scarp represent the record of successive major earthquakes affecting the Central Basin and/or its edges. However, similar sedimentary "events" are not observed in the marine upper part of cores MD01-2429

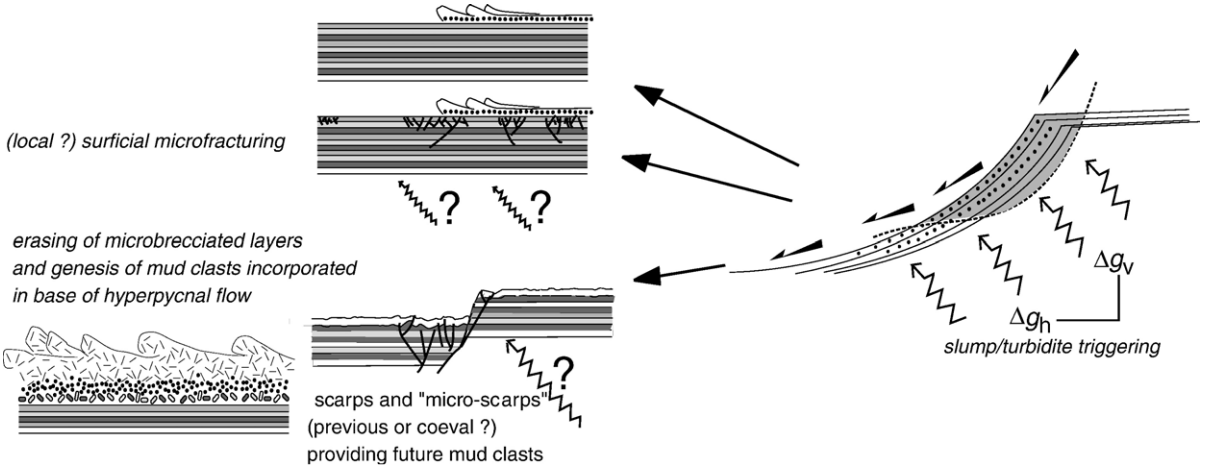

Fig. 13. Schematic genetic model proposed for the underlying mud-clast breccia.

and MD01-2431. This arises the question: what are the processes leading to the similar strong thickness differences between the upper parts of these cores?

4.2. Strong lateral thickness increase in the marine sedimentary sequence

As previously mentioned (Section 3.2), the upper part of the studied sedimentary pile, corresponding to marine sedimentation (12 cal. kyr BP to Present), appears poorly layered and more homogeneous, with very few coarse turbidites. The latter cannot account for the strong thickness increase measured from site MD01-2431 to site MD01-2429 (Fig. 14; location on Fig. 6). Several questions arise:

1) what is(are) the exact depositional process(es) responsible for the general thickness increase on the deeper side of the median scarp of the Central Basin?
2) do the silty laminated episodes (Fig. 15 close-ups) represent particular high terrigenous supply? Do they play the same role as the one attributed to the turbidites/homogenites for the lacustrine sequence (instantaneous huge supply)?

Two sets of data may argue for an explanation: the sediment composition (Section 3.2), and the detailed layering as imaged by X-ray (close-ups, Fig. 15).

The grain size and the mineralogical content of the marine upper sequence indicate a quite continuous supply of silt (and locally fine sand), either as terrigenous suspended load or, more likely, as slow bed-load bottom transport. This sedimentary process must account for at least part of the increased thickness in deepest situation, in a way similar to contourite behaviour, with local bottom current acceleration and subsequent higher particulate transport. A corollary is the question of the relative importance of *in situ* reworking and additional supply. The latter is more in agreement with the sedimentation rate and the grain size.

Another question is the apparent episodic occurrence of siltier, laminated horizons (e.g. Fig. 15a, b and e). These may represent particular climatic episodes with strong run off and connected hyperpycnal distribution. Nevertheless, these laminated units often overlie apparently liquefied fine-grained layers (Fig. 15a, b, c

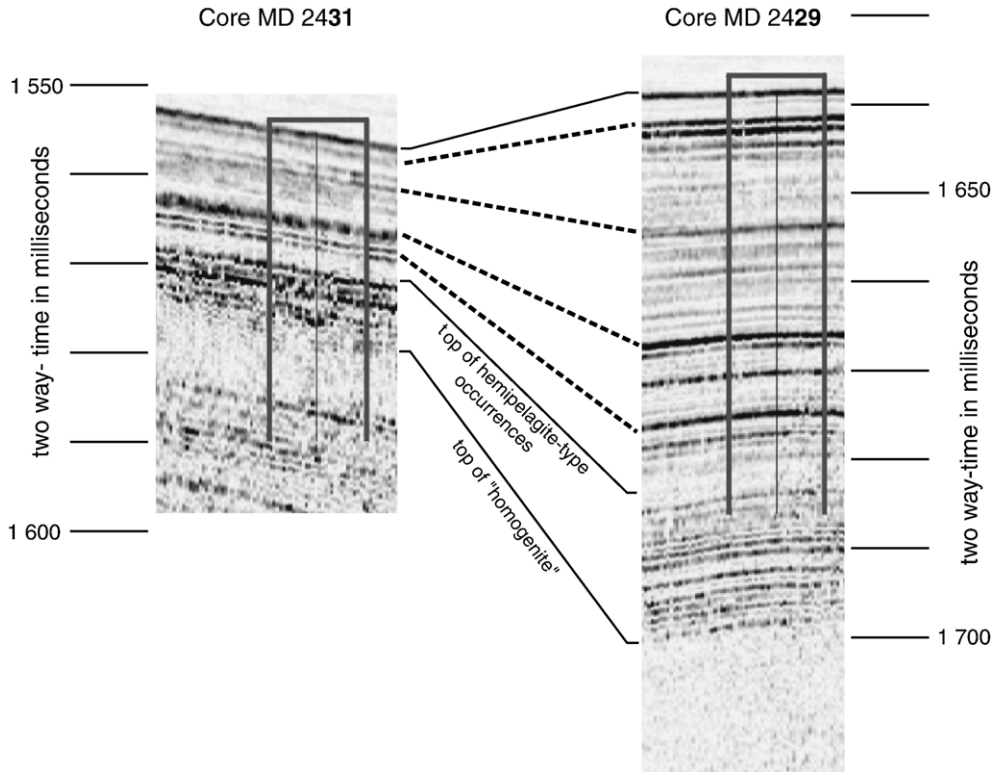

Fig. 14. 3.5 kHz correlations between cores MD01-2429 and MD01-2431 showing, in the whole pile (lacustrine and marine) the thickness increase. For location and depth of the two sites, see Fig. 6.

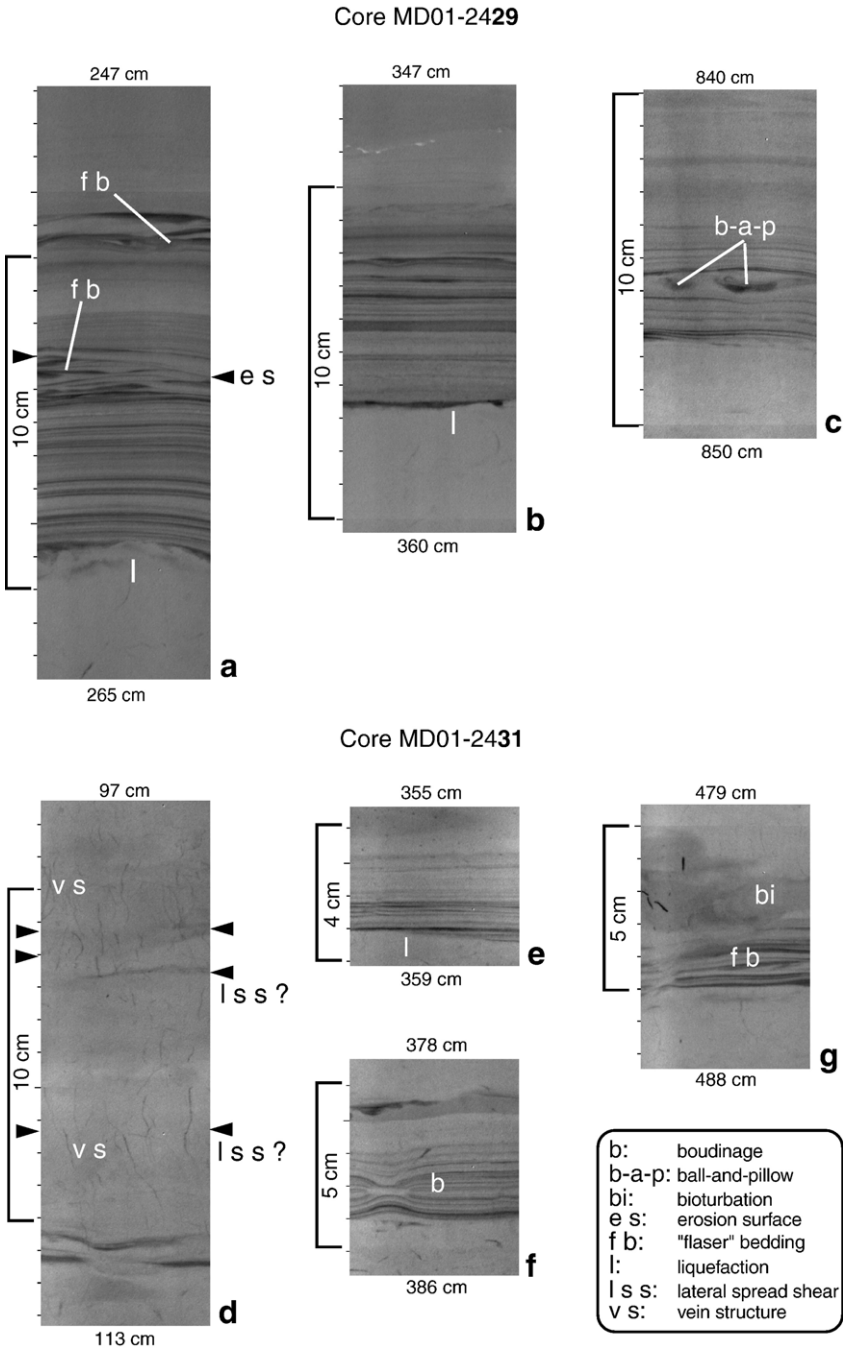

Fig. 15. X-ray SCOPIX close-ups of possible earthquake-related disturbances in the upper (Holocene marine) part of cores MD01-2429 and MD01-2431. Two mechanisms can be deduced: effect of oscillating bottom currents (seiches?) on silt; and water escape with horizontal offsets (lateral shear by shaking?).

and e). Two hypotheses may be proposed: either these units have textures favourable to earthquake disturbances; or they, themselves, represent specific supply induced by major earthquakes. Several features reinforce the first hypothesis (Fig. 15):

1) low angle symmetric cross bedding (similar to coastal tidal "flaser" bedding) is intercalated within the laminated coarser episodes (fb on close-ups, Fig. 15a and g). We interpret these features as induced by to-and-fro bottom displacements, i.e. by

seiche effects due to earthquakes. A "contained turbidite" process cannot be envisaged here.
2) intercalated ball-and-pillow structures (close up, Fig. 15c), also favoured by textural contrasts between superimposed layers during shaking (Moretti et al., 1999).
3) occurrence of water-escape veins starting from these laminated coarser units, with probable associated "boudinage" (close-ups, Fig. 15d and f).

In brief, during the Holocene, the sedimentation appears mainly controlled by rather cyclic episodes of permanent bottom currents with variable suspended load or bedload, depending on the velocity and available silty-sandy terrigenous feeding. The strong lateral thickness variation across the central scarp developed both in a continuous way and by means of separated depositional "events". The later could be responsible for localized development of bioturbation and inferred bottom oxygenation.

4.3. Specific imprints of major earthquakes in the marine sedimentary sequence

For the lower (pre-Holocene) lacustrine sequence (Section 3.4.3), we assumed that the different gravity reworking event deposits (particularly the homogenites) were triggered by major earthquakes during a period of high terrigenous accumulation on the edges of the Sea of Marmara. Microfracturating, which implies a brittle behaviour of unconsolidated sediment with high water content, is also believed to represent a shaking imprint. From tectonic data, seismo-tectonic activity along the North-Anatolian Fault branch is a long term process with no apparent change at the Pleistocene–Holocene boundary. Thus, for the marine upper part of the analyzed sedimentary fill, we should search for other types of imprint of major earthquakes, as the accumulation process is different.

Among the possible earthquake-related features (Fig. 15) we observed:

1) subvertical water-escape "vein structures" (Fig. 15d): these have been described in soft sediments submitted to frequent tectonic and seismo-tectonic activity, as accretionnary complexes (Cowan, 1982; Ogawa and Miyata, 1985; Brown and Berhmann, 1990). As these features are planar (here 2D imaged), they cannot be attributed to bioturbations by worms. An alternative interpretation for these features is the development of bacterial mats, as observed in similar deep dysaerobic conditions by Fossing et al. (1995). Detailed SEM may decipher this.
2) symmetrical flaser bedding-like structures indicating oscillating currents (Fig. 15a) and thus, seiche effects.
3) boudinage of laminated layers (Fig. 15d and f) that we tentatively interpret as lateral spreading effect. This features also resembles the "loop bedding" described by Calvo et al. (1998) and Rodriguez-Pascua et al. (2002), but our observations in split cores are too incomplete to establish the similarity. Some dewatering veins are connected to these stretched layers; however, they are not necessarily genetically linked, because, at a different scale, mud-diapirism is connected to a décollement horizon.
4) horizontal rupturing and displacement of vertical veins (Fig. 15a). We consider these structures as evidence of lateral spread shear, also related to seismic shocks. Such structures have already been interpreted as earthquake imprints in old sedimentary formations (Föhlisch and Voigt, 2001).
5) liquefaction features (Fig. 15a).
6) often an association of these different types.

4.4. Time distribution of sedimentary "events" in the Central Basin's sedimentary record

Gathering visual observations and X-ray pictures of cores MD01-2431 and MD01-2429, the different sedimentary "events" are assumed to be earthquake-triggered and a preliminary rough estimation of their time recurrence intervals is proposed. For the lacustrine part, core MD01-2431 may be divided into a constant "hemipelagic"-type accumulation with a (slow) mean sedimentation rate and intercalated turbidites–homogenites (Figs. 5 and 15), as previously done in deep marine sedimentation by Adams (1990). Between the top of the PLGH and the base of marine sedimentation (16 cal. kyr to 12 cal. kyr BP), the total mean sedimentation rate is about 1.5 mm/yr, implying a 0.15 to 0.30 mm/yr rate for the "hemipelagic"-type sedimentation. Considering this component of the sediment as a planktonic bio-induced and bio-produced settling, then the same rate can be attributed to the "hemipelagic"-type interval of core MD01-2429. In both cores (Fig. 5), these intervals are generally few cm thick; for 2 cm, it should correspond to 35 to 60 yr. About 45 major "events" are visible in core MD01-2431 for a 6-m succession lasting about 4 kyr, leading to a mean 80 yr recurrence time interval.

For the marine part, 6 major events (cf. Fig. 15a) could be correlated between the two cores; adding other types of disturbances and/or particular layering, 26 events occurred during the last 12 kyr leading to a 480 yr mean recurrence interval. The difference observed in apparent

"frequencies" between marine and lacustrine sequences could be explained as follows:

1) only major local earthquakes (directly affecting the Central Basin substratum and its edges) are recorded within the marine part.
2) during Late Glacial (see Section 3.4.3) higher erosion may have driven higher terrigenous supply on the basin margins; weaker compaction related to higher sedimentation rate is thus supposed to decrease the stability and make easier the triggering of subaequous slumps; furthermore the arrival of hyperpycnal flows on the Central Basin deep floor represents a larger provenance area (see submarine canyons pattern on Fig. 6).
3) the estimated "frequency" for the lacustrine sequence is erroneously too high as part of the normal turbidites may be flood turbidites (Lignier, 2001; Arnaud et al., 2002; Beck, in press) and thus rather related to climatic "events" than to earthquake-induced mass wasting.

However, the mean estimated time recurrence interval appears of the same order as the measured recent distribution of major earthquakes along the northern branch of the N.A.F. (Barka and Kadinsky-Cade, 1988; Ambraseys and Finkel, 1991; Stein et al., 1997; Armijo et al., 1999; Hubert-Ferrarri et al., 2000; Barka et al., 2002; Ambraseys, 2002; Armijo et al., 2002). As these historical data concern the whole Sea of Marmara, and farther westwards and eastwards, further more detailed analysis of sedimentary events in the different basins (and not only in the Central Basin) should improve the precision and the validity of our comparison both for chronology and for horizontal distribution.

5. Conclusions: major earthquake control on time and space distribution of the sediments in the Sea of Marmara deep basins

Although based on a detailed study of the unique Central Basin, the following conclusions may be extrapolated to the whole deep part of the Sea of Marmara, as indicated by similar sedimentary piles in all deep cores as well as the high resolution seismostratigraphic succession. The general shape of the recent fill and its internal configuration both evidence a clear control of the deep sedimentary fill by seismic activity.

Regarding the lower lacustrine sequence (approximately from 20,000 cal. yr B.P. to 12,000 cal. yr B.P.), at least 90% of the infilling has to be considered as a non-linear (incremental) process; the maximum instantaneous increment being the pre-Late Glacial Event 8 to 15 m in thickness. This non-linear behaviour appears to work directly in parallel with the co-seismic growth of the vertical component of deep faults. In addition to a deep subaqueous scarp (as for the 1912 event, Armijo et al., 2003, 2005), each major earthquake is supposed to induce coeval gravity reworking, seiche effects, and several other types of sedimentary disturbances mentioned above. Some sedimentary horizons (such as PLGE's top) are reference surfaces for detailed tectonic analysis (Mercier de Lépinay et al., 2003). Conversely, the vertical component of fault scarps often guides the deep co-seismic sediments' arrivals. In addition to some possible seiche effects, the homogenite component (fine-grained suspended load) of the seismoturbidite tends to smooth the created bottom relief. In some cases, the same event can create a deep submarine scarp (tectonic consequence) and immediately erase it (sedimentary consequence).

Concerning the upper marine sequence (12,000 cal. yr B.P. to Present), such non-linear accumulation is not so obvious. The laminated slightly coarser beds appear to have recorded earthquake disturbances but do not clearly represent the impact of seismic events; even so, their relative cumulated thickness does not account for the major part of the successions, nor for the marked lateral thickness increase observed between the two studied sites in the deep Central Basin. As we did not observe repeated true hemipelagic units in this upper part, an apparently continuous silty-sandy flux has to be assumed. An alternative hypothesis is to interpret this monotonous, contrast-lacking, accumulation, as due to the superposition of fine-grained redeposited units that lack directly visible boundaries. Only a highly detailed analysis of the texture and composition of this sequence will enable more precise identification of these postulated events.

Further investigations are in process to improve various proposed interpretations and, overall, determine the time and lateral distribution of major events in the whole Sea of Marmara for the last cal. 20,000 yr; Anisotropy of Magnetic Susceptibility measurements are in process, on both normal sedimentation and major events deposits to check specific particle distribution. Detailed study of Cores 25, 27, and 32, in the other deep basins (Tekirdağ, Kumburgaz, Çinarcic) are in process in order to attempt event-by-event correlation. The detailed analysis of terrigenous fraction (through mineralogy) is also necessary to better define the provenance of reworked material, so as to model huge density current flow trajectories and velocities.

Acknowledgements

The MARMACORE and MARMARASCARPS Cruises were performed within the framework of a French–Turkish scientific collaboration dedicated to the seismic risk in the Istanbul and Sea of Marmara region. These investigations were supported by the Turkish TUBITAK, the French INSU-CNRS, and the French Ministry of Foreign Affairs (MAE). Post-cruise laboratory investigations have been funded be the various involved Laboratories associated to the C.N.R.S. MARMACORE Scientific Team is very grateful to Yvon Balut for successfull management of the giant piston corer. We acknowledge the captain of R/V MARION-DUFRESNE and the whole crew (special thanks to Jean Bart's descendants). We are grateful to J.-M. Daniel, B. Colletta, and J.-M. Mengus for the realization of X-ray scanner images in I.F.P.'s laboratory. D. Gorsline and two anonymous reviewers greatly helped to improve our manuscript.

References

Adams, J., 1990. Paleoseismicity of the Cascadian subduction zone: evidence from turbidites off the Oregon–Washington margin. Tectonics 9 (4), 569–583.

Aksu, A.E., Hiscott, R.N., Yasar, D., 1999. Oscillating Quaternary water levels of the Marmara Sea and vigourous outflow into the Aegean Sea from the Marmara Sea-Black Sea drainage corridor. Marine Geology 153, 275–302.

Aksu, A.E., Hiscott, R.N., Kaminskie, M.A., Mudie, P.J., Gillespie, H., Abrajano, T., Yaşar, D., 2002a. Last glacial-Holocene paleoceanography of the Black Sea and Marmara Sea: stable isotopic, formaminiferal and cocolith evidence. Marine Geology 190, 119–149.

Aksu, A.E., Hiscott, R.N., Yaşar, D., Isler, F.I., Marsh, S., 2002b. Seismic stratigraphy of Late Quaternary deposits fro the southwestern Black Sea relief: evidence for non-catastrophic variations in sea-level during the last 10 000 yr. Marine Geology 190, 61–94.

Alfaro, P., Moretti, M., Soria, J.M., 1997. Soft-sediment deformation structures induced by earthquakes (seismites) in pliocene lacustrine deposits (Guadix-Baza Basin, Central Betic Cordillera). Eclogae Geologicae Helveticae 90, 531–540.

Allen, J.R.L., 1986. Earthquake magnitude–frequency, epicentral distance, an soft sediment deformation in sedimentary basins. Sedimentary Geology 46, 67–75.

Allen, J.R.L., 2001. Principles of Physical Sedimentology. The Blackburn Press. (277 pp.).

Ambraseys, N.N., 2002. The seismic activity of the Marmara sea region over the last 2000 years. Bulletin of the Seismological Society of America 92, 1–18.

Ambraseys, N.N., Finkel, C.F., 1991. Long-term seismicity of Istanbul and the Marmara Sea region. Terra Nova 3, 527–539.

Anand, I., Jain, A.K., 1987. Earthquakes and deformational structures (seismites) in Holocene sediments from the Himalayan–Andaman Arc, India. Tectonophysics 133, 105–120.

Armijo, R., Meyer, B., Hubert, A., Barka, A., 1999. Westward propagation of the North Anatolian Fault into the northern Aegean: timing and kinematics. Geology 27 (3), 267–270.

Armijo, R., Meyer, B., Navarro, S., King, G., Barka, A., 2002. Asymmetric slip partitioning in the Sea of Marmara pull-apart: a clue to propagation processes of the Anatolian Fault. Terra Nova 14, 80–86.

Armijo R., the MARMARASCARPS cruise party (C. Beck, N. Çagatay, Z. Cakir, S. Dominguez, Ö. Emre, K. Eris, L. Gasperini, M.A. Gutscher, E. Hacioglu, C. Imren, I. Lefèvre, J. Malavieille, B. Mercier de Lépinay, B. Meyer, S. Nahirci, B. Natalin, S. Özalaybey, N. Pondard, C. Rangin, K. Sarikavak, S. Schmidt, L. Seeber, L. Tolun, G. Üçarcus), 2003. Young earthquake breaks in the Sea of Marmara floor: a possible underwater extension of the 1912 earthquake rupture? AGU-EGS-EUG Joint Meeting, Nice (April 2003).

Armijo, R., Pondard, N., Meyer, B., Üçarcus, G., Mercier de Lépinay, B., Malavieille, J., Dominguez, S., Gutscher, M.-A., Schmidt, S., Beck, C., Çağatay, N., Cakir, Z., Imren, C., Eris, K., Natalin, B., Özalaybey, S., Tolun, L., Lefèvre, I., Seeber, L., Gasperini, L., Rangin, C., Emre, Ö., Sarikavak, K., 2005. Submarine fault scarps in the Sea of Marmara pull-apart (North Anatolian Fault): Implications for seismic hazard in Istanbul. Geochemistry, Geophysics, Geosystems 6 (6), Q060009. doi:10.1029/2004GC000896.

Arnaud, F., Lignier, V., Revel, M., Desmet, M., Beck, C., Pourchet, M., Charlet, F., Trentesaux, A., Tribovillard, N., 2002. Flood and earthquake disturbance of 210 Pb geochronology (Lake Anterne, NW Alps). Terra Nova 14 (4), 225–232.

Audemard, F., De Santis, F., 1991. Survey of liquefaction structures induced by recent moderate earthquakes. Bulletin of the International Association of Engineering Geology 44, 5–16.

Barka, A., Kadinsky-Cade, K., 1988. Strike-slip fault geometry in Turkey and its influence on earthquake activity. Tectonics 7, 663–684.

Barka, A., et al., 2002. The surface rupture of and slip distribution of the 17 August 1999 Izmit earthquake M 7.4, North Anatolian fault. Bulletin of the Seismological Society of America 92, 43–60.

Beck C., in press. Lacustrine sedimentary records of Late Quaternary seismic activity in the northwestern Alps. Case Studies and Clues for Earthquake-origin Assessment of Sedimentary Disturbances. "Paleoseismology" (McAlpin, Audemard, Michetti, Edts.), Geological Society of America Memoir.

Beck, C., Manalt, F., Chapron, E., Van Rensbergen, P., De Batist, M., 1996. Enhanced seismicity in the early post-glacial period: evidence from the post-würm sediments of Lake Annecy, northwestern Alps. Journal of Geodynamics 22 (1/2), 155–171.

Beck, C., Schneider, J.-L., Cremer, M., Mercier de Lépinay, B., Çagatay, N., Labeyrie, L., Turon, J.-L., Wendenbaum, E., Boutareau, S., Ménot-Combes, G., Hadjas, I., Cortijo, E., MARMACORE Leg Shipboard Scientific Party, 2003. Late Pleistocene major sedimentary reworking event (homogenite) in the Marmara Sea Central Basin: a combination of Late Glacial high terrigenous supply with a major earthquake? Preliminary Results of Giant Piston-coring and High-resolution Seismic Reflection. AGU-EGS-EUG Joint Meeting, Nice (April 2003).

Becker, A., Davenport, C.D., Giardini, D., 2002. Palaeoseimological studies on end-Pleistocene and Holocene around Basle, Switzerland. Geophysical Journal International 149, 659–678.

Becker, A., Ferry, M., Schnellmann, M., Giardini, D., 2005. Multiarchive paleoseismic record of late Pleistocene strong earthquakes in Switzerland. Tectonophysics 400, 153–157.

Ben-Menahem, A., 1976. Dating historical earthquakes by mud profiles of lake-bottom sediments. Nature 262, 200–202.

Bouma, A.H., 2000. Coarse-grained and fine-grained turbidite systems as end members models: applicability and dangers. Marine and Petroleum Geology 17, 137–143.

Boutareaud S., 2003. Etude de l'enregistrement sédimentaire de la sismicité: l'exemple de la Mer de Marmara. Unpublished Master Memoir, University of Bordeaux I.

Bowen, A.J., Normak, W.R., Piper, D.J.R., 1984. Modelling of turbidity currents on Navy Submarine Fan, California continental Borderland. Sedimentology 31, 169–185.

Brown, K.M., Behrmann, J., 1990. Genesis and evolution of small-scale structures in the toe of the Barbados Ridge accretionary wedge. In: Moore, J.C., Mascle, A., et al. (Eds.), Proc. ODP, Sc. Results, vol. 110. Ocean Drilling Program, College Station, TX, pp. 229–244.

Çağatay, N., Görür, N., Algan, O., Eastoe, C.J., Tchapalyga, A., Ongan, D., Kuhn, T., Kuscu, I., 2000. Late Glacial–Holocene paleoceanography of the Marmara Sea: timing of connections with the Mediterranean and the Black Seas. Marine Geology 167, 191–206.

Çağatay, N., Görür, N., Polonia, A., Demirbağ, E., Sakinç, M., Cormier, M.-H., Capotondi, L., McHugh, C., Emre, Ö., Eris, K., 2003. Sea level changes and depositional environments in the Izmit Gulf, eastern Marmara Sea, during the late Glacial–Holocene period. Marine Geology 202, 159–173.

Calvo, J.P., Rodriguez-Pascua, M., Martin-Velasquez, S., Jimenez, S., De Vicente, G., 1998. Microdeformation of lacustrine laminite sequences from Late Miocene formations of SE Spain: an interpretation of loop bedding. Sedimentology 45, 279–292.

Carrillo, E., Audemard, F., Beck, C., Cousin, M., Jouanne, F., Cano, V., Castilla, R., Melo, L., Villemin, T., 2006. A Late Pleistocene natural seismograph along the Boconò Fault (Mérida Andes, Venezuela): the moraine-dammed Los Zerpa paleo-lake. Bulletin of the French Geological Society 177 (1), 3–17.

Carton, H., 2003. Structure of the Cinarcik Basin (eastern Marmara Sea) from densely-spaced multi-channel reflection profiles. Lithos Science Report. Bullard Lab., Univ. of Cambridge, UK, pp. 69–76.

Caselles, J.O., Moretti, M., Alfarao Canas, J.A., Clapès, J., 1997. Estructuras sedimentarias de deformaciòn (sismitas) inducidas por licuefacciòn con un simulador de terremotos. Geogaceta, Sociedad Geológica de España 21, 67–70.

Chapron E., 1999. Contrôles climatique et sismo-tectonique de la sédimentation lacustre dans l'Avant-Pays Alpin (Lac du Bourget) durant le Quaternaire récent. Géologie Alpine, Mémoire H.S. n°30, Univ. J. Fourier, 261 pp.

Chapron, E., Van Rensbergen, P., Beck, C., De Batist, M., Paillet, 1996. Lacustrine sedimentary record of brutal events in Lake Le Bourget (Northwestern Alps–Southern Jura). Quaternaire 7 (2/3), 155–168.

Chapron, E., Beck, C., Pourchet, M., Deconinck, J.-F., 1999. 1822 AD earthquake-triggered homogenite in Lake Le Bourget (NW Alps). Terra Nova 11, 86–92.

Cita, M.B., Rimoldi, B., 1997. Geological and geophysical evidence for a Holocene tsunami deposit in the eastern Mediterranean deep-sea record. Journal of Geodynamics 1–4, 293–304.

Cita, M.B., Camerlenghi, A., Rimoldi, B., 1996. Deep-sea tsunami deposits in the eastern Mediterranean: new evidence and depositional models. Sedimentary Geology 104, 155–173.

Cowan, D.S., 1982. Origin of "Vein Structure" in slope sediments on the inner slope of the Middle America Trench off Guatemala. In: Aubouin, J., von Huene, R., et al. (Eds.), Initial Report Deep Sea Drilling Project, vol. 67. U.S. Govt. Printing Office, Washington, pp. 645–650.

De Batist, M., Imbo, Y., Vermeesch, P., Klerkx, J., Giralt, S., Delvaux, D., Lignier, V., Beck, C., Kalugin, I., Abdrakhmatov, K.E., 2002. Bathymetry and sedimentary environments of Lake Issyk-Kul, Kyrghyz Republic (Central Asia): a large, high-altitude, tectonic lake. In: Klerkx, J., Imanackunov, B. (Eds.), « Lake Issyk-Kul: Its Natural Environment ». NATO Science Series IV, vol. 13. Kluwer Academic Publ., pp. 101–124.

Demirbağ, E., Rangin, C., Le Pichon, X., Şengör, A.M.C., 2003. Investigations of the tectonics of the Main Marmara Fault by means of deep-towed seismic data. Tectonophysics 361, 1–19.

Doig, R., 1985. A method for determining the frequency of large-magnitude earthquakes using lake sediments. Canadian Journal of Earth Sciences 23, 930–937.

Doig, R., 1991. Effects of strong seismic shaking in lake sediments, and earthquake recurrence interval, Temiscaming, Québec. Canadian Journal of Earth Sciences 28, 1349–1352.

Dolan, J., Beck, C., Ogawa, Y., 1989. Upslope deposition of extremely distal turbidites: an example from the Tiburon Rise, west-central Atlantic. Geology 17, 990–994.

El-Isa, Z.H., Mustafa, H., 1986. Earthquake deformations in the Lisan deposits and seismotectonic implications. Geophysical Journal of the Royal Astronomical Society 86, 413–424.

Ergin, M., Bodur, M.N., Ediger, V., 1991. Distribution of surficial shelf sediments in the northeastern and southwestern parts of the Sea of Marmara: straits and canyon regimes of the Dardanelles and Bosphorus. Marine Geology 96, 313–340.

Ergin, M., Kapur, S., Karakas, Z., Akca, E., Kangal, Ö., Keskin, Ş., 1999. Grain size and clay mineralogy of Late Quaternary sediments on a tectonically active shelf, the southern Sea of Marmara: clues to hydrographic, tectonic and climatic evolution. Geological Journal 34, 199–210.

Field, M.E., Gardner, J.V., Jennings, A.E., Edwards, B.D., 1982. Earthquake-induced sediment failure on a 0.25° slope, Klamath River delta, California. Geology 10, 542–546.

Flerit, F., Armijo, R., King, G.C.P., Meyer, B., Barka, E., 2003. Slip partitioning in the Sea of Marmara pull-apart determined from GPS velocity vectors. Geophysical Journal International 154, 1–7.

Föhlisch, K., Voigt, T., 2001. Synsedimentary deformation in the Lower Muschelkalk of the Germanic Basin. In: McCaffrey, W.D., Kneller, B.C., Peakall, J. (Eds.), Particulate Gravity Currents. I.A.S. Publ., vol. 31. Blackwell Science, pp. 279–299 (302 pp.).

Fossing, H., Gallardo, V.A., Jorgensen, B.B., Huttel, M., Nielsen, L. P., Schultz, H., Canfield, D.E., Forster, S., Glud, R.N., Gundersen, J.K., Kuver, J., Ramsing, N.B., Teske, A., Thamdrup, B., Ulloa, O., 1995. Concentration and transport of nitrate by mat-forming sulphur bacterium Thioploca. Nature 374, 713–715.

Gorsline, D.S., De Diego, T., Nava-Sanchez, E.H., 2000. Seismically triggered turbidites in small margin basins: Alfonso Basin, Western Gulf of California and Santa Monica Basin, California Borderland. Sedimentary Geology 135, 21–35.

Guiraud, M., Plaziat, J.-C., 1993. Seismites in the fluvial Bima sandstones: identification of paleoseisms and discussion on their magnitude in a Cretaceous synsedimentary strike-slip basin (upper Benue, Nigeria). Tectonophysics 225, 493–522.

Hempton, M.R., Dewey, J.F., 1983. Earthquake-induced deformational structures in young lacustrine sediments, East Anatolian Fault, southwest Turkey. Tectonophysics 98, 7–14.

Hirn, A., et al., 2003. Elements of structure at crustal scale under the Sea of Marmara from multichannel seismics of the SEISMAR-MARA survey. Geophysical Research Abstracts 13216.

Hiscott, R.N., Aksu, A.E., 2002. Late Quaternary history of the Marmara Sea and Black Sea from high-resolution seismic and gravity-core studies. Marine Geology 190, 261–282.

Hubert-Ferrarri, A., Barka, A., Jacques, E., Nalbant, S.S., Meyer, B., Armijo, R., Tapponier, P., King, G.C.P., 2000. Seismic hazard in the Marmara Sea region following the 17 August 1999 Izmit earthquake. Nature 404, 269–273.

Ĭmren, C., Le Pichon, X., Rangin, C., Demirbağ, E., Ecevitoğlu, B., Görur, N., 2001. The north Anatolian fault within the Sea of Marmara: a new interpretation based on multi-channel seismic and multi-beam bathymetry data. Earth and Planetary Science Letters 186, 143–158.

Kastens, K., Cita, M.B., 1981. Tsunami-induced sediment transport in the abyssal Mediterranean Sea. Geological Society of America Bulletin 92, 845–857.

Komar, P.D., 1971. Hydraulic jumps in turbidity currents. Geological Society of America Bulletin 82, 1477–1488.

Kubo, Y., Yokokawa, M., 2001. Theoretical study on breaking of waves on antidunes. In: McCaffrey, W.D., Kneller, B.C., Peakall, J. (Eds.), Particulate Gravity Currents. International Association of Sedimentologists, Special Publication, vol. 31. Blackwell Science, pp. 65–70.

Kuenen, P.H., 1958. Experiments in geology. Transactions of the Geological Society of Glasgow 23, 1–28.

Le Pichon, X., Sengor, A.M.C., Demirbag, E., Rangin, C., Imren, C., Armijo, R., Gorur, N., Çağatay, N., Mercier de Lépinay, B., Meyer, B., Saatcilar, R., Tok, B., 2001. The active main Marmara Fault. Earth and Planetary Science Letters 192, 595–616.

Lignier V., 2001. Les sédiments lacustres et l'enregistrement de la paléoséismicité.Etude comparative de différents cas dans le Quaternaire des Alpes Nord-Occidentales et du Tien-Shan Kyrghize. Unpublished Doct. Thesis, University of Savoy.

Lignier, V., Beck, C., Chapron, E., 1998. Caractérisation géométrique et texturale de perturbations synsédimentaires attribuées à des séismes, dans une formation quaternaire glaciolacustre des Alpes (les «Argiles du Trièves"). Compte-Rendu de l'Académie des Sciences, Paris 327, 645–652.

Major, C., Ryan, W., Lericolais, G., Hajdas, I., 2002. Constraints on Black Sea outflow to the Sea of Marmara during the last glacial-interglacial transition. Marine Geology 190, 19–34.

Marco, S., Agnon, A., 1995. Prehistoric earthquake deformations near Masada, Dead Sea Graben. Geology 23 (8), 695–698.

McClusky, S., Bassalanian, S., Barka, A., Demir, C., Ergintav, S., Georgiev, I., Gurkan, O., Hamburger, M., Hurst, K., Hans-Gert, H.-G., Karstens, K., Kekelidze, G., King, R., Kotzev, V., Lenk, O., Mahmoud, S., Mishin, A., Nadariya, M., Ouzounis, A., Paradissis, D., Peter, Y., Prilepin, M., Relinger, R., Sanli, I., Seeger, H., Tealeb, A., Toksöz, M.N., Veis, G., 2000. Global positioning system constraints on plate kinematics and dynamics in the eastern Mediterranean and Caucasus. Journal of Geophysical Research 105, 5695–5719.

Mercier de Lépinay B., Labeyrie L., Çağatay N., MARMACORE Scientific Team, 2001. IFRTP unpublished shipboard report, 34 p.

Mercier de Lépinay, B., Labeyrie, L., Çağatay, N., Beck, C., Schneider, J.-L., Cremer, J.-L., Turon, Londeix, L., Meyer, M., Gallet, Y., Pondard, N., Ménot-Combes, G., Hajdas, I., Cortijo, E., 2003. Interplay between recent sedimentation and active tectonics in Marmara Sea. AGU-EGS-EUG Joint Meeting, Nice (April 2003).

Moretti, M., Tropeano, M., 1996. Strutture sedimentarie deformative (sismiti) nei depositi tirreniani di Bari. Memori della Societa. Geologica Italiana 51, 485–500.

Moretti, M., Alfaro, P., Caselles, O., Canas, J.A., 1999. Modelling seismites with a digital shaking table. Tectonophysics 304, 369–383.

Mörner, N.-A., 1996. Liquefaction and varve deformation as evidence of paleoseismic events and tsunamis. The autumn 10,430 BP case in Sweden. Quaternary Science Review 15, 939–948.

Mulder, T., Cochonat, P., 1996. Classification of offshore mass movements. Journal of Sedimentary Research 66 (1), 43–57.

Mulder, T., Tisot, J.-P., Cochonat, P., Bourillet, J.-F., 1994. Regional assessment of mass failure events in the Baies des Anges, Mediterranean Sea. Marine Geology 122 (1/2), 29–45.

Nakajima, T., Kanai, Y., 2000. Sedimentary features of seismoturbidites triggered by the 1983 and older historical earthquakes in the eastern margin of the Japan Sea. Sedimentary Geology 135, 1–19.

Nemec, W., 1990. Aspects of sediment movement on steep delta slopes. In: Colella, A., Prior, D.B. (Eds.), Particulate Gravity Currents. International Association of Sedimentologists, Special Publication, vol. 10. Blackwell Science, pp. 29–73.

Obermeier, S., 1989. The New Madrid earthquakes: an engineering-geologic interpretation of relict liquefaction features. U.S. Geological Survey Professionnal Paper, 1336-B. 114 pp.

Obermeier, S.F., Bleuer, N.R., Munson, C.A., Munson, P.J., Martin, W.S., McWilliams, K.M., Tabaczynski, Odum, J.K., Rubin, M., Eggert, D.L., 1991. Evidence of strong earthquake shaking in the lower Wabash valley from prehistoric liquefaction features. Science 251, 1061–1063.

Ogawa, Y., Miyata, Y., 1985. Vein structure and its deformation history in the sedimentary rocks off the Middle America Trench off Guatemala. Initial Report Deep Sea Drilling Project, vol. 84. U.S. Govt. Printing Office, Washington, pp. 811–829.

Okay, A.I., Kaslilar-Ozcan, A., Imren, C., Botzepe-Guney, A., Demirbag, E., Kuscu, I., 2000. Active faults and evolving strike-slip fault basins in the Marmara Sea, northwest Turkey: a multichannel reflection survey. Tectonophysics 312, 189–218.

Pickering, K.T., Hiscott, R.N., 1985. Contained (reflected) turbidity currents in the Middle Ordovician Cloridorme Formation, Québec, Canada: an alternative to the antidune hypothesis. Sedimentology 32, 373–394.

Piper, D.J.W., Cochonat, P., Ollier, G., Le Drezen, E., Morrison, M., Baltzer, A., 1992. Evolution progressive d'un glissement rotationnel en un courant de turbidité: cas du séisme de 1929 des Grands Bancs (Terre Neuve). Compte-Rendu de l'Académie des Sciences, Paris 314, 1057–1064.

Plaziat, J.-C., Purser, B.H., Philobbos, E., 1988. Diversity of Neogene seismites of the NW Red Sea (Egypt): a characteristic sedimentary expression of rifting. Tectonophysics 153, 295.

Pratt, B.R., 1998. Syneresis cracks: subaqueous shrinkage in argillaceous sediments caused by eathquake-induced dewatering. Sedimentary Geology 117, 1–10.

Rangin, C., Demirbag, E., Imren, C., Crusson, A., Normand, A., Le Drezen, E., Le Bot, A., 2001. Marine Atlas of the Sea of Marmara (Turkey). IFREMER2-84433-068-1.

Ringrose, P.S., 1989. Paleoseismic (?) liquefaction event in late Quaternary lake sediments at Glen Roy, Scotland. Terra Nova 1, 57–62.

Rodriguez-Pascua, M.A., Calvo, J.P., De Vicente, G., Gòmez-Gras, D., 2002. Soft-sediment deformation structures interpreted as seismites in lacustrine sediments of the Prebetic Zone, SE Spain, and their potential use as indicators of earthquake magnitudes during the Late Miocene. Sedimentary Geology 135 (1–4), 117–135.

Roep, T.B., Everts, A.J., 1992. Pillow-beds: a new type of seismite? An example from an Oligocene turbidite fan complex, Alicante, Spain. Sedimentology 39, 711–724.

Ryan, W.B.F., Pitman, W.C., Major, C.O., Shimkus, K., Moskalenko, V., Jones, G.A., Dimitrov, P., Görür, N., Sakinç, M., Yüce, H., 1997. An abrupt drowning of the Black Sea shelf. Marine Geology 138, 119–126.

Séguret, M., Labaume, P., Madariaga, R., 1984. Eocene seismicity in the Pyrénées from megaturbidites of the South Pyrenean basin (Spain). Marine Geology 55, 117–131.

Seilacher, A., 1984. Sedimentary structures tentatively attributed to seismic events. Marine Geology 55, 1–12.

Shiki, T., Kumon, F., Inouchi, Y., Kontani, Y., Sakamoto, T., Tateishi, M., Matsubara, H., Fukuyama, K., 2000. Sedimentary features of the seismo-turbidites, Lake Biwa, Japan. Sedimentary Geology 135, 37–50.

Siegenthaler, C., Finger, W., Kelts, K., Wang, S., 1987. Earthquake and seiche deposits in Lake Lucerne, Switzerland. Eclogae Geologicæ Helveticæ 80, 241–260.

Sims, J., 1973. Earthquake-induced structures in sediments of Van Norman Lake, San Fernando, California. Science 182, 161–163.

Sims, J., 1975. Determining earthquake recurrence intervals from deformational structures in young lacustrine sediments. Tectonophysics 29, 141–152.

Stanley, D.J., 1981. Unifites: structureless muds of gravity-flow origin in Mediterranean basins. Geo-Marine Letters 1, 77–83.

Stanley, D.J., Maldonado, A., 1981. Depositional models for fine-grained sediments in the western Hellenic Trench, Eastern Mediterranean. Sedimentology 28, 273–290.

Stein, R.S., Barka, A., Dieterich, J.H., 1997. Progressive failure on the North Anatolian Fault since 1989 by earthquake stress triggering. Geophysical Journal International 128, 594–604.

Stow, D.A.V., Wetzel, A., 1990. Hemiturbidite: a new type of deep-water sediment. Proceeding of the Ocean Drilling Program 105B, 25–34.

Stuiver, M., Reimer, P.J., Bard, E., Beck, J.W., Burr, G.S., Hugen, K.A., Kromer, B., McCormac, G., Van der Plicht, J., Spurk, M., 1998. INTCAL 98 Radiocarbon age calibration, 24 000–0 cal BP. Radiocarbon 40, 1041–1083.

Syvitski, J.P.M., Schafer, C.T., 1996. Evidence for an earthquake-triggered basin collapse in Saguenay Fjord, Canada. Sedimentary Geology 104, 127–153.

Tolun, L., Çağatay, M.N., Carrigan, W.J., 2002. Organic geochemistry and origin of Late Glacial–Holocene sapropelic layers and asociated sediments in Marmara Sea. Marine Geology 190, 47–60.

Tuttle, M., Seeber, L., 1991. Historic and prehistoric earthquake-induced liquefaction in Newbury, Massachusetts. Geology 19, 594–597.

Van Loon, A.J., Brodzikowski, K., Zielinski, T., 1995. Shock-induced resuspension deposits from a pleistocene proglacial lake (Kleszczow graben, central Poland). Journal of Sedimentary Research 65 (2), 417–422.

Vittori, E., Labini, S., Serva, L., 1991. Paleoseismology: review of the state of the art. Tectonophysics 193, 9–32.

Wong, H.K., Lüdmann, T., Ulug, A., Görür, N., 1995. The Sea of Marmara: a plate boundary sea in an escape tectonic regime. Tectonophysics 244, 231–250.

Yalçiner, A.C., Alpar, B., Altinok, Y., Özbay, İ., Imamura, F., 2002. Tsunamis in the Sea of Marmara historical documents for the past, models for the future. Marine Geology 190, 445–463.